An Analysis of Partial-Depth, Floating, Impermeable Guidance Structures for Downstream Fish Passage at Hydroelectric Facilities

Hydro Research Foundation

Final Report

Presented by

Kevin Mulligan

Environmental and Water Resources Engineering

Department of Civil and Environmental Engineering

University of Massachusetts Amherst

December 2014

Contents

Preface

The following chapters are submitted to the Hydro Research Foundation (HRF) as a Final Report on the findings made by Kevin Mulligan. The focus is on partial-depth, floating, impermeable guidance structures (FIGS) for downstream fish passage at hydroelectric facilities. The work began in August 2013 and was completed in December of 2014. Chapter 1 and Chapter 2 are written as papers that are to be submitted for publication, covering the computational fluid dynamics modeling (Chapter 1) and physical modeling (Chapter 2) efforts. Chapter 3 describes the work that is to be completed between Jan and May 2015 which focuses on both potential improvements to the FIGS design and the sensitivity of the flow field to parameters not yet investigated. Prior to submittal at a peer-reviewed journal each chapter will be reviewed by Kevin Mulligan's PhD Committee, consisting of Dr. Brett Towler (HRF project advisor, US Fish and Wildlife Service / UMass Amherst), Dr. Alex Haro (US Geological Survey / UMass Amherst), and Dr. David Ahlfeld (UMass Amherst). The HRF will be sent a copy of each paper after the editing process is complete and each chapter is submitted for publication. The HRF will also be notified if a paper is successfully published.

In addition, I would like to thank the Hydro Research Foundation for supporting my research over the past year and a half. It was truly a wonderful experience getting to know all those involved in the HRF, including the other fellows. It has allowed me to pursue a career in fish passage engineering that otherwise would not have been possible. Please let me know if there is anything I can do to help support the foundation going forward.

Chapter 1: A review of floating impermeable guidance structures and how their design parameters effect the flow field

1. Abstract

A floating impermeable guidance structure (FIGS) for downstream fish passage is constructed as a series of partial-depth panels anchored across a river channel, reservoir, or power channel. If guidance is successful, the fish will avoid entrance to a dangerous intake structure (i.e. turbine intakes) while passing from the upstream to downstream end of a dam through a safer passage route (i.e. the bypass). To evaluate the flow field immediately upstream of a FIGS, a parameterized CFD model of an idealized power channel was constructed in ANSYS Fluent v. 14.5. The design parameters investigated were the angle and depth of the FIGS and the average approach velocity in the power channel. Key findings indicate that a FIGS set at a small angle and deep enough such that the Effective Guidance Depth of the FIGS is greater than the expected vertical distribution of fish approaching the structure will perform the best.

2. Introduction

Many fish species have evolved to use different types of environments over their life span in order to enhance the population's chance of survival. Each selected environment is well suited for a particular part of the life cycle for the fish. For instance, clupeids (such as American Shad and river herring) are born in a fresh water river system where there are fewer predators, migrate as juveniles to the ocean where there is a larger food supply, then migrate as adults back to the fresh water river to spawn, restarting the cycle. Fish species that exhibit this life cycle are referred to as anadromous, and the clupeids are one of many. Without the ability to freely move between and within each aquatic ecosystem, the chance of an anadromous fish population's long-term survival is greatly diminished (Limburg and Waldman, 2009; McDowall, 1987).

As a result of anthropogenic influences on river systems, full and partial barriers to fish movement exist in very high numbers in watersheds worldwide. These barriers consist of small to large size dams, culverts, and other structures. While some man-made barriers are now obsolete and provide no benefit to society, many exist which do provide a great utility. By providing flood control, water supply security, and/or hydroelectricity, dams can create a very valuable resource. However, passage of fish both up and downstream of dams can be difficult to impossible. Even if a fishway structure is in place, poor design, predation, and degraded water quality (among others) can lead to fatigue, injury, fatality, or other hindrances to fish survival.

Due to these complications, many fish species are often unable to complete their typical life cycle and are now considered threatened or endangered (Hall et al., 2012). In the United States, environmental regulations have increasingly focused on the conservation and restoration of aquatic ecosystems. For instance, Atlantic salmon have been listed as an endangered species and in 2011 NOAA was petitioned to list some alosines (blueback herring, alewife) as endangered.

Alosines are already a priority species on the east coast of the United States for numerous state and federal resource agencies (e.g. NOAA, USFWS). The clear biological need for safer passage, the species that are already endangered, and the recent petitions incentivizes the enhancement of downstream passage efficiencies at hydropower facilities. These incentives are not only confined to the east coast of the United States, fish are anadromous in both the southern and northern hemispheres (McDowall, 1987) and many of these same problems exist throughout the globe. Improvements to surface guidance technologies (SGT) (e.g., louvers, racks, screens, perforate plates, impermeable panels) that lead to bypasses may prove a more cost-effective way to protect these increasingly important and threatened fish. The aim of this paper is to review floating impermeable guidance structures (FIGS) and to provide a detailed assessment on how the structure's design parameters impact fish passage.

The remainder of the paper is outlined as follows: Section 3 will provide background on the FIGS; Section 4 will focus on the construction of a CFD model encompassing the region immediately upstream of a FIGS; Section 5 will provide the results of the CFD modeling efforts; Section 6 will discuss the results and the limitations of this work; and Section 7 will summarize the paper.

3. Background

At a typical hydropower facility there are three primary routes of downstream passage for a fish. The three routes, ordered by typical proportion of total river flow, are 1) through the turbine intakes, 2) over a spillway at the dam and 3) through a fish bypass (often constructed as a sluice gate, weir, or pipe). To reduce the number of fish passing through the turbine intakes, the fish bypass is constructed in close proximity to the turbine intakes. The challenge is to either induce behaviorally or actively guide the fish into the bypass rather than the turbine intakes, which the bulk of the flow in the power channel passes through (typically >90% when there is no spilling over the dam). The SGT's, and in particular the FIGS's, are used for this purpose. Depending upon the configuration of the hydroelectric facility, the SGT's will be placed in the river channel or the constructed power channel. A FIGS is intended to increase safe passage of downstream migrating surface-oriented fish species, such as salmonids and alosines.

Johnson and Dauble (2006) classified the flow upstream of a typical hydroelectric facility as consisting of three separate zones. The first zone an outmigrating fish will enter is the "Approach Zone", located about 100-10,000 m upstream of the dam. Here salmonid and alosine juveniles are expected to follow the bulk flow while remaining in the upper portion of the water column (Whitney et al., 1997; Buckley and Kynard, 1985; Faber et al., 2011). Key features within this zone include channel depth, channel shape, discharge, shoreline features, and current pattern. The fish movement typically includes both actively swimming and passively drifting.

Next is the "Discovery Zone", located about 10-100 m from the dam, where the fish are expected to encounter the flow net of the surface bypass and turbine intakes. Key features here include the

forebay bathymetry, structures, velocity gradients (from spill and turbine loading), sound, and light. In this zone, the fish begin to respond to the site specific conditions of the hydroelectric facility. Johnson et al. (2005) showed that the horizontal distribution for juvenile salmonids can be impacted by dam operations in this zone and Venditti et al. (2000) showed that fish tend to spend more time in this zone than they would normally.

Next is the "Decision Zone", located about 1-10 m from the dam. Key features here that impact fish behavior are velocity, acceleration, turbulence, strain, sound, light, structures, and other fish (Larinier, 1998). Within this zone, the turbine intakes creates a strong downward flow component and the surface bypass can elicit strong acceleration. As evidenced by Haro et al. (1998), Kemp et al. (2005), Johnson et al. (2000), and Taft (2000), several juvenile fish species prefer to avoid regions of high acceleration. It is imperative that the fish be entrained in the flow net of the bypass before any of these features stimulate an avoidance reaction and that the hydraulic conditions through the bypass is safe for the fish to travel. It is the goal of the FIGS to alter the flow in the "Decision Zone", and partially the "Discovery Zone", such that adult and particularly juvenile surface-oriented anadromous fish are actively guided to a downstream surface bypass or collection system.

Figure 1: Partial-depth, floating, impermeable guidance structure. The photo on the left (provided by Shane Scott) shows the panels with the floating boom. The photo on the right (taken from Google Earth) shows an installed guidance device at the Bonneville Dam.

A FIGS (Fig. 1) is constructed of a series of floating partial-depth impermeable panels anchored across a river channel, reservoir, or power channel (Scott, 2012). According to Scott (2012), the design is based off of the knowledge that: 1) juvenile anadromous fish tend to swim in the top portion of the water column (Whitney et al., 1997; Buckley and Kynard, 1985; Faber et al., 2011), 2) some juvenile species have been shown to select a shallow rather than deep passage route when given the choice (Johnson et al., 1997), and 3) anadromous juveniles tend to migrate downstream in the river thalweg (Whitney et al., 1997).

To the author's knowledge, the first study and implementation of an impermeable guidance structure was in 1995 at the Bellows Falls Dam on the Connecticut River in Vermont, U.S.A. (TransCanada Hydro Northeast Inc., 2012). Studies in 1991, 1992, and 1994 all indicated that

Atlantic salmon smolts tended to pass through the turbine intakes rather than the ice/debris sluice bypass. This triggered the construction of the partial-depth, 62.8 meter long, 4.6 meter deep (at normal impoundment elevation), fixed concrete guidance structure at a 45 degree angle to the flow in 1995. A radio telemetry study in that year's migration season proved that the device was highly effective by actively guiding 94% of the smolts to the bypass (Hanson, 1999; TransCanada Hydro Northeast Inc., 2012). The TransCanada report indicates the structure is still in use as of 2012.

Following the work at Bellows Falls Dam, the first FIGS was installed at the Lower Granite Dam on the Snake River in Washington, U.S.A. in 1998. Adams et al. (2001) explains that the FIGS was a steel wall 330 meters long and 17-24 meters deep angled towards a surface bypass collector immediately upstream of the turbine intakes. The FIGS impact on fish passage was examined using biotelemetry and hydro-acoustic techniques. The study showed that mean residence times in the forebay for chinook salmon, hatchery steelhead, and wild steelhead increased by 1.6, 1.7, and 2.4 times when the FIGS was absent than when it was present. In addition, fish passage efficiency was significantly increased when the FIGS was present than when it was absent causing the authors to believe this is a viable option to improve downstream passage of anadromous fish.

In 2009, NextEra Energy constructed and installed a 4 foot deep, 300 foot long FIGS in the Lockwood power canal in Maine, U.S.A (NextEra Energy Maine Operating Services, LLC, 2010) on the Kennebec River. The FIGS consisted of an impervious rubber material and attached to the bottom was 6 feet of 7/16 inch Dyneema netting. While NextEra Energy was testing the FIGS for its resistance to tearing, debris loading, and other structural issues, they observed juvenile clupeids being guided to the fish bypass at the terminus of the FIGS. However, they also observed juveniles on the downstream side of the FIGS that either sounded under the FIGS or passed through tears in the structure. Later, in 2010, the FIGS was replaced due to structural issues by a new guidance device. A Brookfield White Pine Hydro LLC (2014) report describes the new device as a 10 foot deep permeable structure. The two panels closest to the bypass entrance are a perforated plate and the panels further upstream are a combination of 4 foot deep perforated plate and 6 foot deep netting. These types of permeable structures are common because they reduce the force being applied on the structure by allowing some water to pass through and can be more buoyant. However, the sweeping flow along the guidance device is reduced and the approach flow perpendicular to the device is increased which can cause impingement and/or entrainment. Perforated plate guidance devices installed at three hydropower facilities in the Kennebec River watershed (Weston, Hydro Kennebec, and Lockwood) effectively guided approximately 65% of Atlantic Salmon smolts to the site's respective bypass (personal communication, Bob Richter).

In 2010, the Tacoma Power Utilities released a report (Tacoma Public Utilities, 2010) evaluating a FIGS at Cowlitz Falls Dam on the Cowlitz River in Washington, U.S.A. The FIGS is composed of a 4 feet deep screen panel and attached below that was a 15 feet deep tarp panel. The goal of the FIGS at this site is to guide fish to a surface collector in order to trap and transport outmigrating fish to downstream of the dam. The study evaluated juvenile steelhead, coho, and Chinook using acoustic telemetry. Over 90% of the fish entering the forebay at this site did not exhibit direct movement along the FIGS to the collector, rather they meandered for over 4 hours in the forebay before passing. However, the distribution of fish in the forebay clearly showed that most of the time was spent upstream of the FIGS, implying the structure was able to influence the fish behavior. The report states that overall the FIGS showed promise for influencing the behavior of outmigrants and that more fish than expected arrived at the terminus of the FIGS (76 to 93% by species), but improvements are needed. The study identified the following possible areas for future evaluation: positioning the collector entrance at the FIGS terminus, increasing attraction flow into the collector, extending the depth of the FIGS, and increasing it rigidity to maintain a vertical orientation. Later, in 2011, the United States Geological Survey released a report (Kock et al., 2012) on a radiotelemetry evaluation performed in that year studying again juvenile salmonids at the Cowlitz Falls Dam. The guidance structure evaluated in 2010 was replaced by a 10 foot deep, solid steel plate FIGS. 40 to 63% of the fish by species arrived at the fish collection discovery area and movement patterns showed that the FIGS was effective at guiding fish along the device. However, the movement patterns also showed that the fish had a strong tendency to sound under the FIGS and on to the turbine intakes where 33 to 52% of the fish by species passed downstream (the largest percentage of all the passage routes).

More recently, the US Army Corps of Engineers released a report in 2011 (Faber et al., 2011) evaluating a FIGS impact on the passage and survival of juvenile salmonids (yearling Chinook salmon, subyearling Chinook salmon, and juvenile steelhead) at the Bonneville Dam located on the Columbia River at the border of Oregon and Washington, U.S.A. The FIGS in this study is 700 feet long and 10 feet deep. The report is based off of an acoustic-telemetry study and shows that the FIGS improves collection efficiency and effectiveness for the yearling Chinook salmon but no discernable difference was noted for the other two fish species when compared to prior years testing. Important to note from this study is that between 45-50% of the fish that passed through the turbines went under the FIGS to get there. The other 50% went on gaps on the north and south side of the structure. This indicates that the design could likely be altered to reduce the number of fish passing below and around the structure.

Ongoing in 2014, the California Department of Water Resources (CA DWR) is studying FIGS's for use in the Sacramento River located in California, U.S.A. The purpose of the FIGS is to prevent outmigrating juvenile salmonids in the Sacramento River from being entrained into the Georgiana Slough. Lab scale physical modeling was performed and the researchers found that

the FIGS panels oriented at 22 degrees to the flow resulted in neutrally buoyant beads guiding along and not passing under the FIGS (personal communication, Shane Scott). The CA DWR is testing a 5 feet deep FIGS at this angle in situ using radio tagged fish. Results are pending.

Several other studies have been performed using computational fluid dynamics (CFD) as a means to better understand how a FIGS will impact the flow field in a forebay. The U.S. Army Corps of Engineers released a report in 2006 (Rakowski et al., 2006) studying the impact of a FIGS in the forebay of the Dalles Dam located on the Columbia river which borders Oregon and Washington, U.S.A. The report looked at a 40 feet deep FIGS set at 30 degrees and another at 45 degrees from the face of the powerhouse, each starting in the same upstream location. If juvenile outmigrating fish follow the streamlines alone, then in most scenarios it was shown that the FIGS will not be successful in guiding fish. However, as previously noted, juvenile anadromous fish prefer to stay in the top portion of the water column. Thus it is imperative that the downward flow component is not strong enough to force the fish underneath the structure and likely on to the turbines. The study showed that streamlines briefly flow along the structure then pass under and enter into a helical recirculation pattern along the backside. Interestingly, at the Bonneville Dam FIGS fish have been entrained in this recirculation and guided to the bypass (Scott, 2012). As stated in the U.S. Army Corps of Engineers report, the extent of helical recirculation is influence by the depth and angle of the structure. This study also evaluated the minimum acceptable length of the FIGS for this specific site. CFD simulations were performed for 20, 30, and 40 feet depths. The 40 feet deep structure performed the best when comparing streamlines from the terminus of the FIGS to the preferred route of passage. However, this is a site specific recommendation and it will depend upon the location of the preferred route of passage for outmigrating fish. It was also noted that the location of the downstream end of the FIGS is critical as even small changes can greatly impact the streamlines that begin at the terminus of the structure.

Another CFD approach to studying a FIGS was performed by Lundstom et al. (2010). The authors examined FIGS in the Pite River in Sweden upstream of a spillway and turbine intakes at a hydroelectric facility. The goal of the FIGS was to direct the surface oriented juvenile smolts towards the spillway instead of the turbine intakes. The authors studied 10 FIGS configurations with different lengths (80 to 144 meters), curvatures (straight, bend in downstream end, full bend with small radius, full bend with large radius, etc.), and depths (1.7 to 2.5 meters). The study found that the FIGS performed best at low spilling rates and the device should stretch over a major part of the width of the river. An important metric used in this analysis was the acceleration along the FIGS and the acceleration downward upstream of the FIGS. The authors argued that a high acceleration downward upstream of the FIGS would improve guidance efficiencies because several other papers have shown that juveniles tend to avoid regions of high acceleration, as previously discussed. The authors were satisfied with the performance of the FIGS because the acceleration along the device was much smaller than that going downward,

meaning the fish would choose the route along the device. While this may be true in certain cases, we argue caution because a downward acceleration that is too high may entrain the weak swimming juvenile fish and force them under the FIGS towards the turbines, as shown in NextEra Energy Maine Operating Services, LLC (2010), Kock et al. (2012), and Faber et al. (2011). An additional finding from the Lundstrom et al. (2010) article was that the vertical velocity (z) component was affected at depths greater than twice that of the FIGS, but the horizontal (x and y) components were mostly unaffected by the FIGS at depths below it.

There is a pressing need for technological innovations in the hydropower industry that can protect threatened aquatic species while maintaining efficient levels of hydropower production. A FIGS can help achieve these objectives, however, more research is needed to understand how the key design parameters (depth and angle in particular) effect the flow field and improve or deter fish passage. Novel to this study is the examination of the flow field upstream of a FIGS that is set at a wide range of depths and angles to flow and subject to a wide range of average approach velocities, all within an idealized power channel. Also novel to this study are the metrics used to evaluate the results.

4. Idealized CFD Model

Model Domain

To evaluate the flow field immediately upstream of a FIGS, a parameterized CFD model of an idealized power channel was constructed in ANSYS Fluent (ANSYS Inc., 2012). Fig. 2 displays the plan view of the power channel and a cross sectional view from the furthest downstream location at the bypass entrance. The gray hatched area in the plan view represents the model domain. The section downstream of the FIGS was not modeled to simplify the analysis. To accurately model head losses that are incurred by the structure a more complex model than is presented here is required.

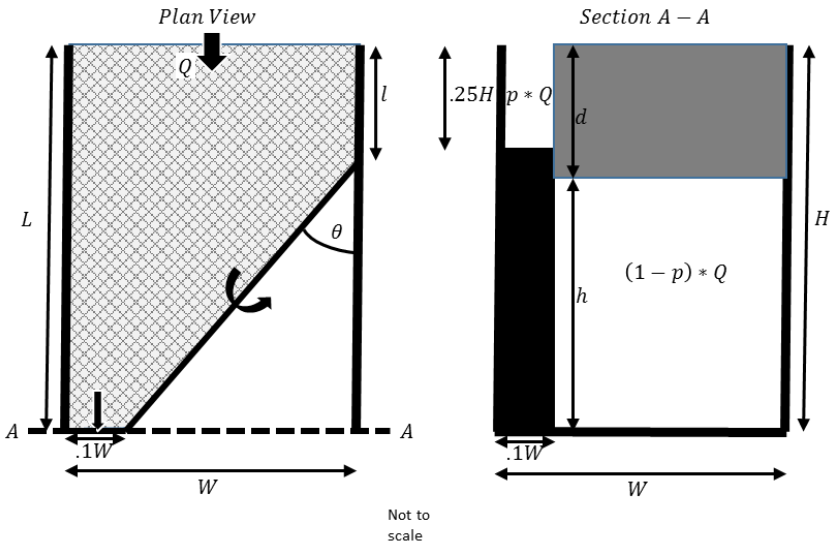

Figure 2: The schematic on the left shows the plan view of the idealized power channel. The hatched area (upstream of the FIGS and bypass entrance) is the modeled region. The schematic on the right shows the cross-sectional view from A-A, the furthest downstream location as seen on the plan view. The grey area is the guidance structure. The black area is the wall directly below the bypass entrance.

For each scenario, the inlet location is fixed and the approach distance ℓ is held constant at 25 feet. The total length of the model, L, varies according to the angle of the guidance structure, θ. The channel width, W, is 100 feet and the channel depth, H, is 40 feet. The width of the bypass is .1W or 10 feet. The depth of the bypass opening is .25H or 10 feet. The percent of the total flow through the bypass, p, is 5%.

Model Parameters

The key parameters relevant to this work are the depth of the FIGS, d, the angle of the FIGS, θ, and the average inlet velocity, V. Table 1 displays the ranges and intervals each parameter is evaluated on:

Table 1: Model parameter ranges and intervals

Parameter	Range	Interval
Depth of the FIGS (d), ft	5 to 20	5
Angle of the FIGS (θ), deg	25 to 45	10
Average Inlet Velocity (V), fps	2 to 4	2

Each of these ranges were decided upon by applying both the author's own experiences and values reported in the literature. There are 24 total scenarios.

Boundary Conditions

Three different types of boundary conditions (BC) are used in each of the model scenarios.

The first type of BC is a velocity inlet. The inlet is defined using a velocity profile of a fully developed flow with an average inlet velocity, V. The velocity profile for V = 4 fps is shown in Fig. 3. To attain each developed flow profile, a rectangular channel CFD model was constructed, termed the Inlet Calculation CFD Model (ICCM). The ICCM used a cross section at the inlet of the Idealized CFD Model and

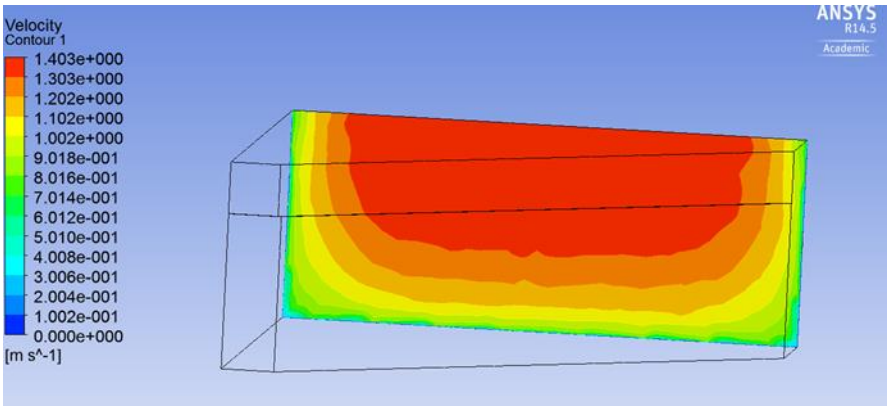

Figure 3: The contour plot on the inlet of the CFD model geometry represents the velocity specified as a BC in the case of V = 4 fps. Note the fully developed flow profile.

extruded it long enough such that fully developed flow could be achieved. In each ICCM run, the inlet was set to a uniform velocity equal to V and the outlet was specified as an outflow carrying 100% of the flow. Identical solvers, described later, were used for both the ICCM runs and the Idealized CFD Model. The velocity profile at the outlet of the ICCM is used as the velocity profile at the inlet of the Idealized CFD Model. In addition to the velocity profile, the turbulence intensity is specified at 5%. ANSYS Fluent recommends the use of 5% in the event this value is unknown, as it is in this case.

The second type of BC is an outflow outlet. The outlet is defined in two locations: 1) directly under the FIGS and 2) through an entrance to a bypass. The two white areas in the cross-section A-A for Fig. 2 depicts each of the BC locations. Each outlet is prescribed a percent of the total outflow, previously defined as p. The CFD model calculates the velocity, pressure, and turbulence profile at the outlets given the percent of flow through each outlet.

The third type of BC is a wall condition with a specified shear and roughness height value. The water surface is defined as a slip-condition with a specified shear stress of zero and zero roughness. The channel walls and bottom are defined as a no slip condition, with a defined roughness height in the range of a smooth concrete. The face of the FIGS is also defined as a no-slip condition, but the roughness height is about half of the roughness height of the walls. The FIGS exterior is often composed of a rubber or stainless steel.

Mesh

In all scenarios for both the Idealized CFD Model and the ICCM, the domains were divided into a number of finite volumes in the form of tetrahedrons. Face and body sizing rules were applied in different regions of the domain. The smallest cells occur near the boundaries and guidance structure. Inflation layers were used to accurately model the wall roughness effects on the flow field. The inflations layers were applied at all boundaries of the model, including the guidance structure. The aspect ratio, orthogonal quality, and skewness were the primary metrics used to evaluate mesh quality. Number of elements ranged from approximately 350,000 to 512,000.

Solver and Convergence Criteria

All CFD runs performed in this analysis use the second order upwind method to solve the conservation of momentum equations for steady-state conditions. The runs are solved using the SIMPLE scheme as the pressure-velocity coupling method. The realizable k-Ɛ model with standard wall functions is used to describe the turbulent kinetic energy and turbulent dissipation rate. Similar to momentum, the turbulence model is solved using the second order upwind method. However, in all scenarios each model was first solved using the first order upwind scheme. The results of the first order upwind solving scheme were used as the initial solution to the second order upwind solver. This provided a means to reach convergence quicker. Convergence criteria included the equation residuals for continuity, x-velocity, y-velocity, z-

velocity, turbulent kinetic energy, and turbulent dissipation rate. Additional monitors included the integral of the velocity magnitude on the outlet below the FIGS, integral of velocity magnitude on the outlet to the bypass, total volume integral of the velocity magnitude in all fluid cells, the integral of the skin friction coefficient on the guidance face, and the total volume integral of turbulent kinetic energy in all fluid cells. Details regarding the conservation of momentum and turbulence solvers can be found in the ANSYS Fluent v. 14.5 code documentation manual (ANSYS Inc., 2012).

5. Results

To compare the 24 total scenarios, two metrics are formulated based on each scenario's velocity output. The two metrics are titled the Volume of Exceedance (VOE) and the Work Indicator (WI).

The Volume of Exceedance reports the volume of space above a depth of d* (ranging from 5 to 40 ft in 5 ft intervals) within each scenario's model domain that exceeds a specified velocity magnitude. The VOE is intended to act as a surrogate for the probability that a single fish will encounter velocities that exceed its swim speed capacity at some point along its travel through the specified region of the model domain. Fig. 4 and Fig. 5 display the VOE (y-axis) versus the specified velocity magnitude (x-axis) for scenarios where the Average Inlet Velocity, V, is equal to 2 fps (Fig. 4) and 4 fps (Fig. 5). Eight plots are shown within each figure corresponding to different d* values. The vertical gold line represents V and the vertical purple line represents the maximum velocity at the inlet of the model domain. With no FIGS, the VOE for velocities greater than the maximum inlet velocity (purple line) would likely be close to zero. Therefore, a VOE greater than 0 for velocity magnitudes greater than the maximum inlet velocity provides an indication that the FIGS is resulting in velocities higher than what is typical within the power channel.

Fig. 4 and Fig. 5 illustrate the effect of the depth and angle on the velocity magnitudes within each model domain. It is shown that for velocities greater than the maximum inlet velocity (purple line) the depth of the structure, d, is the prominent parameter affecting the VOE, followed by the angle, θ. If d* = 40 ft (and thus the entire model domain is used to calculate the VOE) the maximum VOE in this high velocity range corresponds to the scenario of d = 20 ft and $\theta = 45°$, whereas the minimum VOE corresponds to the scenario of d = 5 ft and $\theta = 25°$. The same patterns emerge for both V values. However, as d* is reduced the scenarios corresponding to the max VOE values in this high velocity range begins to shift. At d* = 20 ft, the maximum VOE values pertain to the scenarios of d = 15 ft and $\theta = 45°$. At d* = 15 ft, the maximum VOE values pertain to the scenarios of d = 10 ft and $\theta = 45°$. At d* = 10 ft, the maximum VOE values pertain to the scenarios of d = 5 ft and $\theta = 45°$. It becomes clear that the relative performance of each configuration is dependent upon d*, making clear the importance for understanding the vertical distribution of fish approaching the structure.

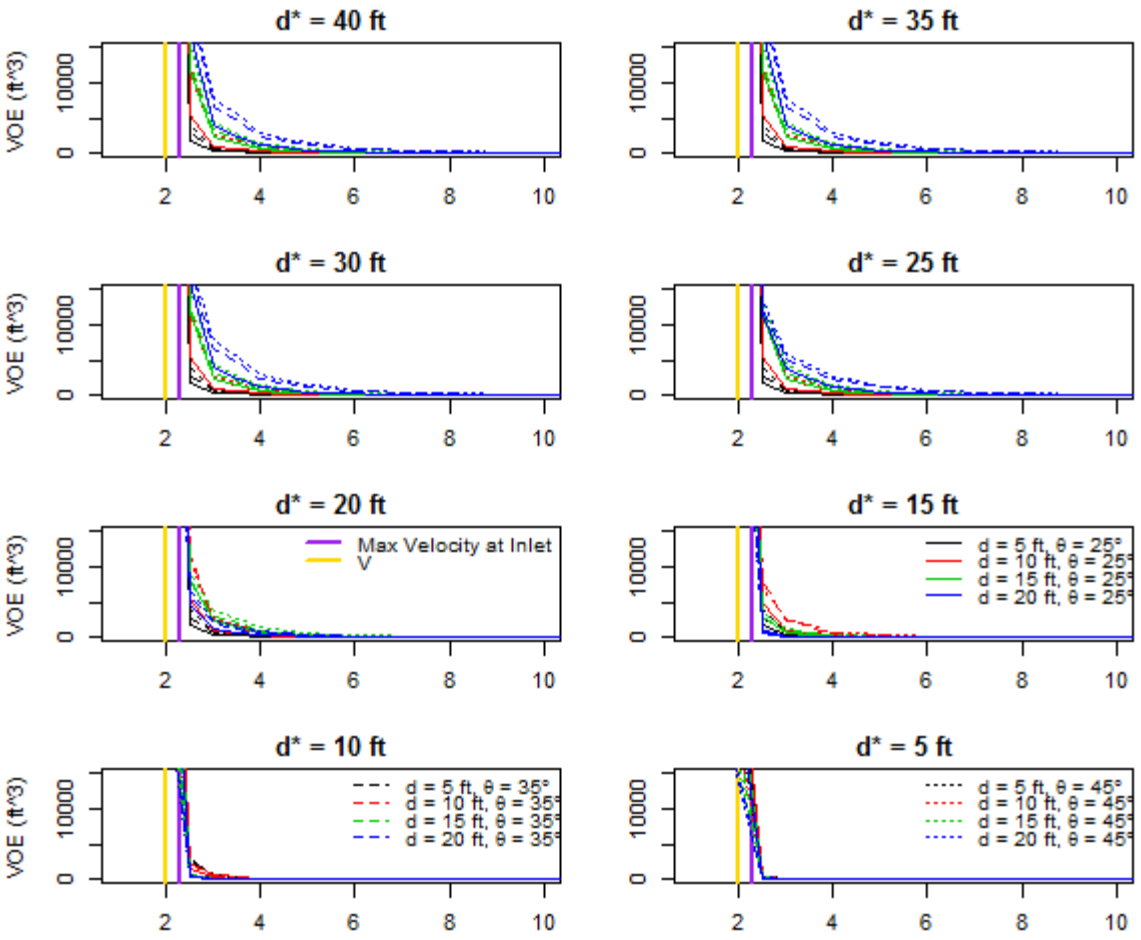

Figure 4: The VOE is plotted against the velocity magnitude for V = 2 fps and multiple d* values. The vertical purple line indicates the maximum velocity at the inlet. The vertical gold line indicates the Average Inlet Velocity, or V.

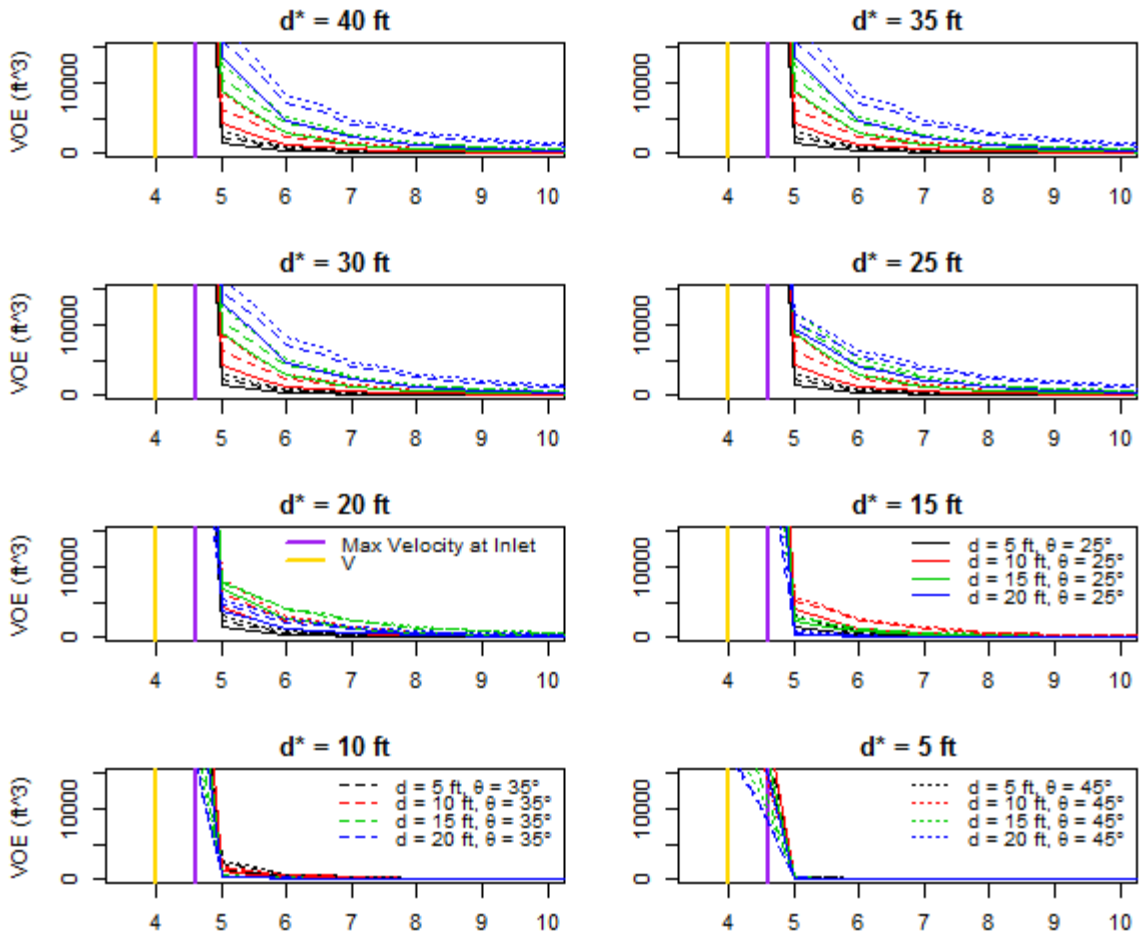

Figure 5: The VOE is plotted against the velocity magnitude for V = 4 fps and multiple d* values. The vertical purple line indicates the maximum velocity at the inlet. The vertical gold line indicates the Average Inlet Velocity, or V.

The VOE is useful because in addition to Fig. 4 and Fig. 5, we are also able to evaluate VOE values corresponding to the swimming speed capability of different fish species at different life stages. For example, the VOE values in Fig. 6 below pertain to the minimum Adult American Shad prolonged (4 fps) and sprint (8 fps) swim speeds according to Bell (1990) for d* = 40 ft. We compare the prolonged speed to the configurations where V is equal to 2 fps and the sprint speed to the configurations where V is equal to 4 fps. In effect, the VOE here reports the domain volume that exhibits velocities twice that of V, or the average inlet velocity. We chose American Shad because the species are relatively weaker swimmers than other possible target species (i.e. salmonids) and we chose the adult life stage because the minimum juvenile fish swimming speeds are significantly less than both V values used in this analysis.

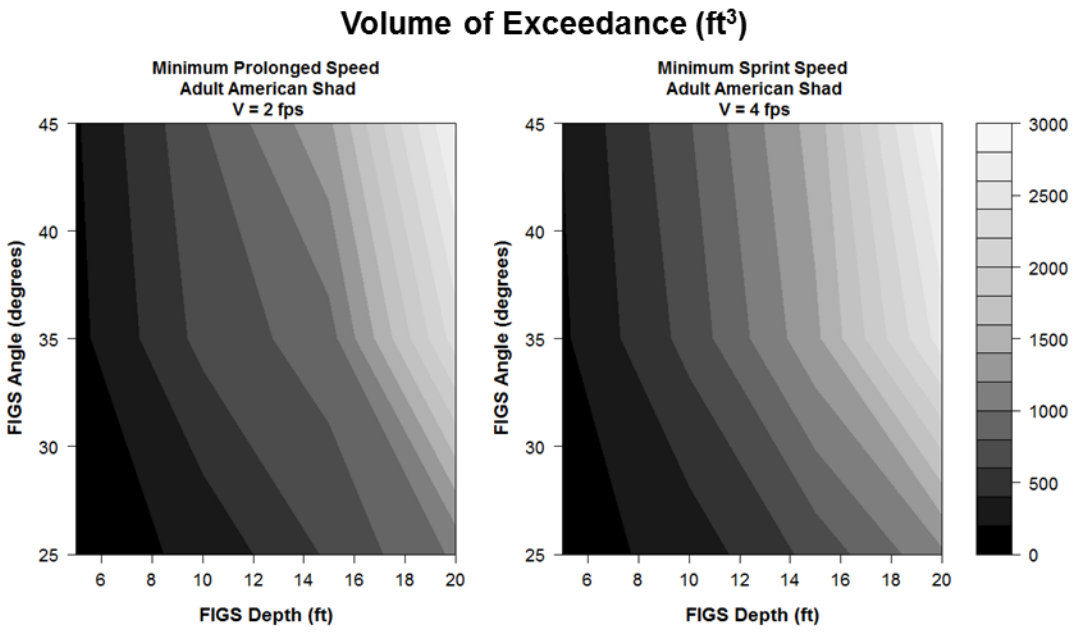

Figure 6: Contour plots of the Volume of Exceedance for the FIGS depth versus angle where d* = 40 ft. The plot on the left shows the VOE corresponding to the minimum prolonged speed for adult American Shad (4 fps) for the scenarios of V = 2 fps. The plot on the right shows the VOE corresponding to the minimum sprint speed for adult American Shad (8 fps) for the scenarios of V = 4 fps.

Once again, the effect of the angle and depth of the guidance structure on the velocity magnitudes in the model domain are clearly on display. Logically, as the depth of the FIGS increase, the VOE increases. This occurs because the flow is forced through a smaller cross sectional area, thereby increasing velocities. Perhaps counterintuitive, as the angle decreases (creating a larger model domain volume) the VOE also decreases. This decrease in VOE occurs despite the embedded handicap for shallower angles in this metric. Consequently, multiple tradeoffs exists regarding changes in the depth and/or angle of the FIGS. For instance, increasing the depth of the FIGS (thereby attempting to provide guidance for fish swimming at greater depths) increases the corresponding VOE (thereby possibly reducing guidance efficiency). Another example is decreasing the angle of the FIGS. This will reduce the VOE but will also increase the length of the FIGS potentially causing the fish to swim a longer distance along the structure.

Next is the Work Indicator, or WI. As the name implies, this metric does not calculate the actual work a fish would exert when swimming along a FIGS. Instead, it uses the velocity of the water squared (the primary variable for drag force on a still object in water) and an assigned path to provide an indicator of the guidance difficulty for a fish swimming along the FIGS to the bypass at a specified depth. The fish is assumed to be attempting to oppose the flow field over the entire path length. This metric is used instead of calculating the actual work because when doing so

many uncertainties arise (drag coefficient, swim path, orientation, etc.) and is thus outside the scope of this paper.

The WI is found by taking the integral of the velocity of the water squared along the path using numerical integration. The path we assign begins at a worst-case location, far away from the bypass entrance at the inlet of the model on the opposite side of the power channel and at the water surface. We use the streamline from that starting point as computed by ANSYS Fluent. The typical path, shown in Fig. 7, travels along nearly the full length of the guidance structure ending at the bypass. A streamline path similar to the one shown in Fig. 8 is determined for each model scenario.

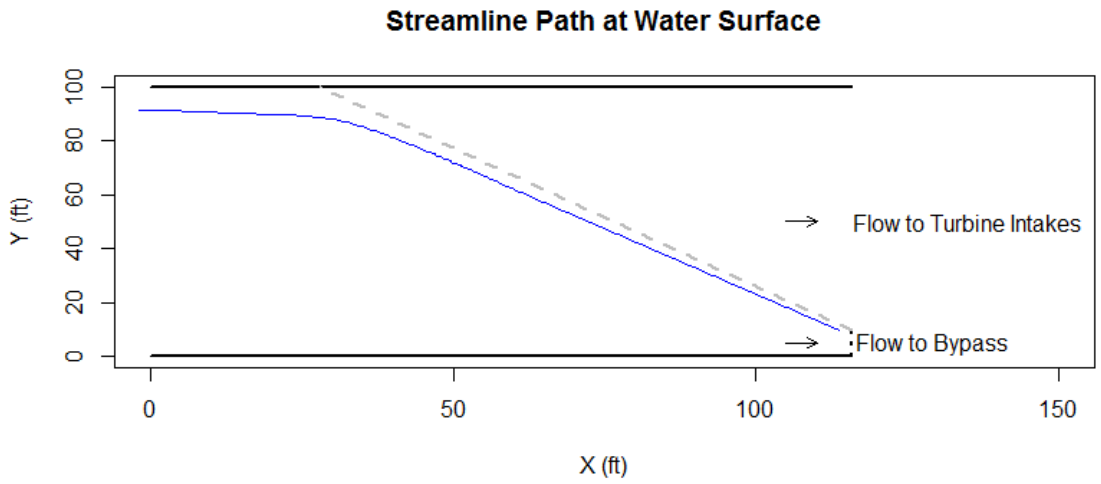

Figure 7: A typical streamline path at the water surface (blue line). The grey dashed line is the guidance structure. Flow is from left to right.

We apply this same path in the x and y plane along different depths of the model domain from the water surface to the bottom of the FIGS, called the Pathway Elevation, regardless of the velocity encountered. Once the depth of the path is below the bypass entrance (Elevation of 30ft), an adjustment to the path depth must be made such that the path ends at the bypass. For the purposes of this paper, the path increases elevation up to the bypass at a location very close to it (within 5 feet). This means that the path will remain at the assigned path depth until it is within 5 feet of the bypass, at which point it will rise linearly to the center of the bypass.

The WI also provides a useful way to 1) compare the WI corresponding to each of the flow components, and 2) prescribe an Effective Guidance Depth (EGD), as evidenced in Fig. 9 (for V=2fps) and Fig. 10 (for V=4fps). The EGD is equal to the elevation where the gradient of WI_z (the WI corresponding to the z-velocity component) is above a threshold value of 50 ft^2/s^2. This threshold value was determined through a trial and error process with a goal of finding the value where the WI_z begins to increase rapidly. Using this threshold value, the region above the bottom of the FIGS can be broken into two zones, the Effective Guidance Zone (grey), EGZ, and

the Ineffective Guidance Zone (white), IGZ. Here we assume that the downstream migrating fish prefer the region where the downward flow component is low and relatively constant, compared to the rapidly increasing values towards the bottom of the FIGS. This likely gives fish the best chance to be guided along the structure and not swim underneath it. As previously documented in the Background Section, many fish have been documented swimming or being entrained underneath these structures. The strong downward flow is likely the most problematic feature of a FIGS.

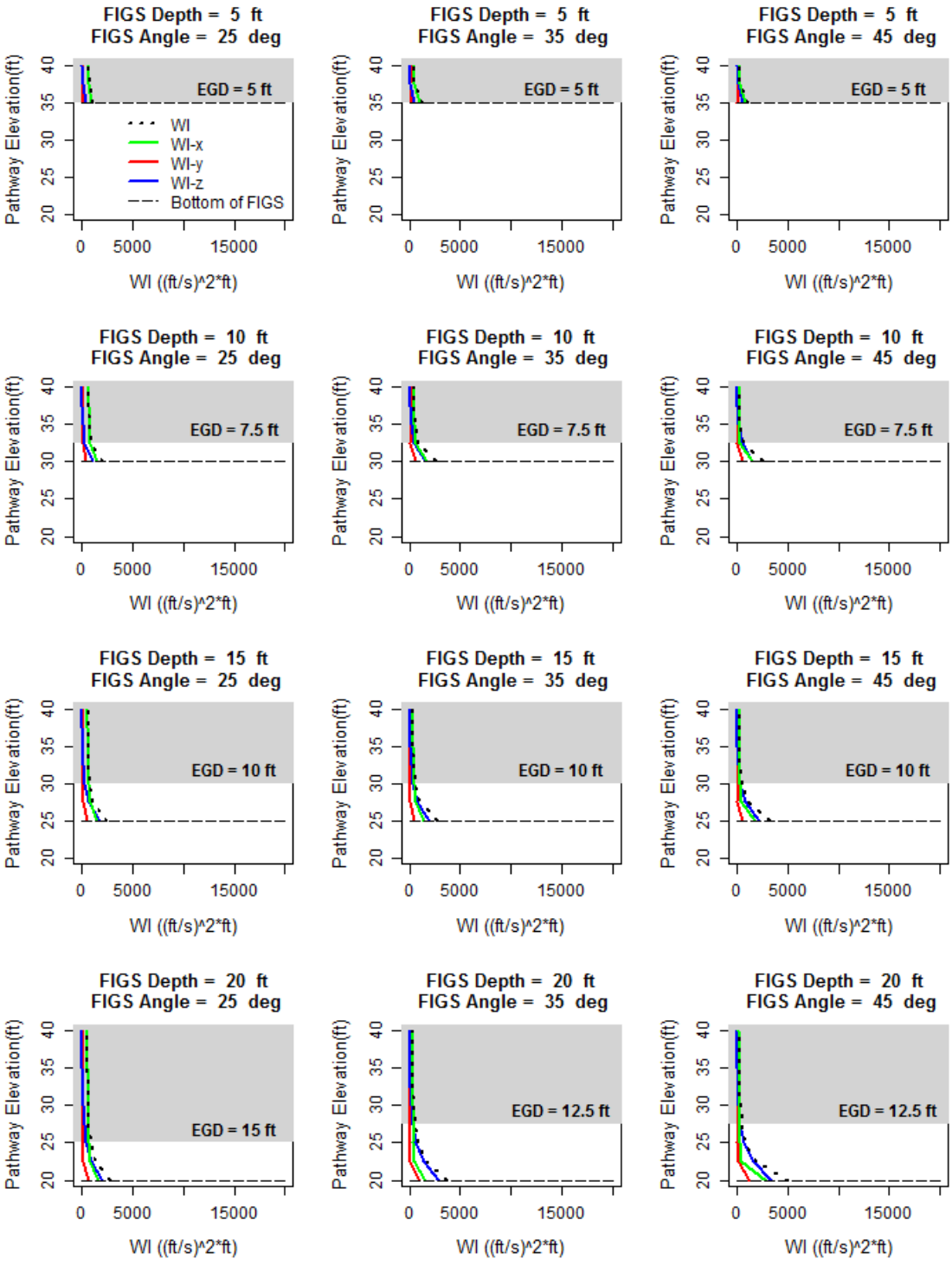

Figure 8: The Pathway Elevation (ft) is plotted against the Work Indicator (ft/s)2*ft, WI, for each model scenario where V = 2 fps. The dotted line indicates the magnitude of the WI. The green, red, and blue lines indicates the WI corresponding the x-velocity, y-velocity, and z-velocity components. The dashed line represents the bottom of the FIGS at depth d. The grey region illustrates the Effective Guidance Zone.

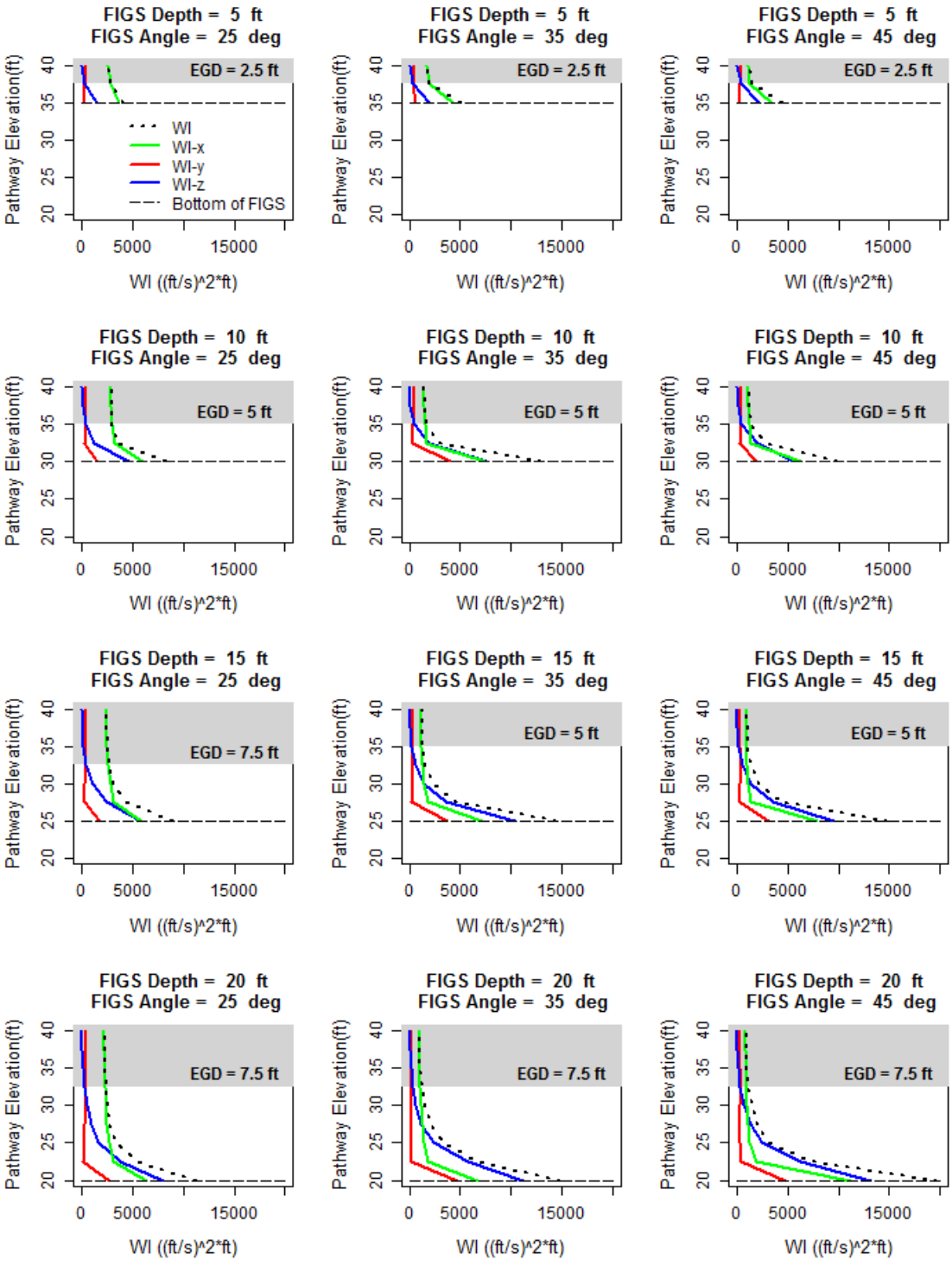

Figure 9: The Pathway Elevation (ft) is plotted against the Work Indicator (ft/s)2*ft, WI, for each model scenario where V = 4 fps. The dotted line indicates the magnitude of the WI. The green, red, and blue lines indicates the WI corresponding the x-velocity, y-velocity, and z-velocity components. The dashed line represents the bottom of the FIGS at depth d. The grey region illustrates the Effective Guidance Zone.

We find several important takeaways from Fig. 8 and Fig. 9. First, the WI peak always occurs at the very bottom of the FIGS. For d = 5 or 10 ft, WI-x tends to be greater than WI-y and WI-z at the WI peak. However, as the depth is increased and d = 15 or 20 ft, WI-z is greater than both WI-x and WI-y at the WI peak. Thus as fish swim along the bottom of a FIGS set at a deeper elevation, they may be more likely to follow the flow underneath the FIGS. Second, the WI peak value is reduced as the angle is reduced, despite the fact that a lower angle results in a longer path length. This occurs because the velocities at the bottom of the FIGS in the larger angle configurations is considerably higher than in the smaller angles. Fig. 8 and Fig. 9 also show consistently that within the top 10 feet of the water column the WI values decrease as the angle is increased. This opposite effect takes place because the velocities for the smaller and larger angles at these elevations are similar but the length of the path is much shorter for the larger angles. Third, an average inlet velocity of 2 fps creates much more passable conditions than when V = 4 fps, as evidenced by the much larger WI values and the greatly reduced EGD's. For an average inlet velocity of 4 fps, the fish are much more likely to either volitionally follow the downward velocity component or be entrained by it. And fourth, deepening of the FIGS will increase both the EGD and the size of the IGZ. This relationship means that for an increase in d there will not be an equal increase in the EGD.

6. Discussion

The results of each of the metrics show conflicting indications of which configuration is best.

For the VOE, a smaller angle and a smaller depth tends to be the best, but when taking into account the vertical distribution of the approaching fish this result changes. In particular, a FIGS depth of 5 feet, while performing well in terms of the VOE, will in most cases be insufficient to guide the majority of fish. Despite that, if the vertical distribution of fish is within the top 5 ft. of the water column then a guidance structure set at 5 ft. will likely perform as well as a deeper structure according to the VOE. If the vertical distribution of fish is within the top 10 ft. of the water column, then a structure depth of 15 or 20 ft. provides only slight gains when compared to the VOE results of the 10 ft. deep structure. If the expected vertical distribution is within the top 15 feet of the water column then a structure depth of 20 ft. performs the best. If the expected vertical distribution is within the top 20 feet of the water column then a structure depth of 20 ft. is the only option presented that could possibly guide all the fish to the bypass. However, an increase in depth of the structure is likely to provide gains as shown in the previous scenario.

For the WI, a deeper structure tends to be the best whereas the best angle choice is less apparent. While the peak WI values are greater for deeper structures, these peak values occur outside of the EGZ. The primary concern is increasing the EGD, which a deeper structure accomplishes. Furthermore, a larger angle results in a smaller WI value in the EGZ, meaning if the structure is designed such that the majority of fish will approach the structure in this zone, the larger angle will create a shorter path and may result in less fatigue if the fish attempts to oppose the flow. However, if fish approach the guide wall at a depth deeper than expected, the advantage of a

larger angle is lost and the fish will have less of a chance of being safely guided to the bypass than if the angle was smaller. Also, it's not clear that the difference in WI values for a change in angle at a fixed depth is large enough to warrant a greater angle, particularly when considering 1) the peak WI values are much higher for greater angles and 2) the VOE values are much larger for greater angles. In addition, the ratio of WI-z to WI increases as the angle is increased, meaning that as the angle is increased 1) juvenile fish which either passively drift with the flow of water or use their weak swimming capacity will be more likely to be entrained below the guide wall and 2) adult fish following their negative rheotactic behavior will be more likely to swim below the guide wall.

Considering the information gleaned from the VOE and the WI, the authors recommend using a deeper structure at a smaller angle. In particular, the most preferred option is a configuration which exhibits lower peak velocities along the face of the structure (particularly the z-component of velocity) and that is deep enough such that the EGD is greater than the extent of the expected vertical distribution of all the target fish species at the site. Although it is important to note that the optimal design does not have an angle approaching zero degrees. The cost of such a structure along with the constructability of one would make it infeasible.

We fully acknowledge the limitations that existed upon conducting this research. Namely, the use of CFD model is on its own an uncertain science. When compared to the real world the CFD results are bound to differ. It is in the hands of the modeler to ensure that difference will be as small as possible. In addition, the CFD models used in this paper are of an idealized power canal, are not representative of a real site, and are therefore not calibrated to any real world results. Consequently, the results of this analysis rely greatly on an accurate description of the boundary conditions, the discretized mesh, and the second order solvers. Furthermore, the use of a single phase model results in a loss of model resolution near the water surface boundary layer, although this is not expected to make a substantial difference in the results.

Without testing fish movement in situ, it is difficult to predict how a fish will respond to the flow conditions. Although we formulated metrics to try and circumvent this problem, the results can in no way estimate actual fish behavior and they depend upon a few key assumptions. First, Fig. 6 showing the VOE in respect to American Shad swim speeds is dependent upon the Bell (1990) reference, although that, at least in some cases, has been shown to be inaccurate (Castro-Santos, 2005). Fortunately, the Bell (1990) data appear to be a conservative estimate of swimming capabilities, and so we remain comfortable using this approach. Second, the WI relies on a prescribed path. We recognize that the path we prescribed is not the path a fish would take. There is plenty of evidence showing that fish tend to meander, and so their total swimming length would be much longer than the path we prescribe. However, we believe it is a useful indicator for the relative difference in effort a fish would need to perform as it swims along the face of a FIGS in an orientation opposing the flow along the path. Third, each of the metrics

developed are based off of the velocity output data from the CFD analysis. Other key hydraulic features that impact fish behavior include acceleration, turbulence, and strain (Larinier, 1998). Inclusion of these variables could make for a more sound approach to understanding how fish will behave near the FIGS.

Other physical aspects of the structure have been ignored. The forces applied to a FIGS creates a vertical tilt such that the guidance wall is not perpendicular to the water surface. In addition, a curvature often develops when looking from plan view. Ideally, strengthening of the structure and anchoring it to the bottom could minimize the deflection. But because the degree of vertical tilt and horizontal curvature will vary from site to site, the author's decided to use no tilt or curvature in the model, again striving for an idealized setting to perform the analysis. Although the author's do not believe either effect will cause drastic changes in the results.

7. Conclusion

Impermeable guidance structures have been utilized to improve downstream passage survival for anadromous fish including salmonids and alosines over the past 20 years. Less implemented than other surface guidance technologies (e.g. louvers, bar racks, screens, among others), they are gaining popularity, particularly in the north western United States. This body of research focuses on the key design parameters and begins to answer the question of which configuration is best for fish guidance. A CFD approach is used to answer this fundamental question. The key findings indicate that a FIGS set at a small angle and deep enough such that the EGD is greater than the expected vertical distribution of fish approaching the structure will perform the best. Future work is necessary, particularly to calibrate the CFD model and perform more rigorous testing in situ with the various fish species of interest.

8. Acknowledgements

The information, data, or work presented herein was funded in part by the Office of Energy Efficiency and Renewable Energy (EERE), U.S. Department of Energy, under Award Number DE-EE0002668 and the Hydro Research Foundation.

9. Disclaimer

10. References

Adams, N. S., Johnson, G. E., Rondorf, D. W., Anglea, S. M., & Wik, T. (2001). Biological evaluation of the behavioral guidance structure at Lower Granite Dam on the Snake River, Washington in 1998. *American Fisheries Society Symposium, 26*, 145-160.

ANSYS, Inc. (2012). *ANSYS FLUENT theory guide.* Canonsburg, PA: Southpointe.

Bell, M. (1990). *Fisheries handbook of engineering requirements and biological criteria.* U.S. Army Corps of Engineers, North Pacific Division. Fish Passage Development and Evaluation Program.

Brookfield White Pine Hydro LLC. (2014). *Adaptive management plan for downstream passage of GOM DPS Atlantic salmon at the Weston (FERC No.2325), Shawmut (FERC No.2322) and Lockwood (FERC No.2574) Projects on the Kennebec River and the Brunswick project (FERC No.2284) on the Androscoggin River.*

Buckley, J., & Kynard, B. (1985). *Vertical distribution of juvenile American Shad and Blueback Herring during the seaward migration in the Connecticut River.* Massachusetts Cooperative Fishery Research Unit, Department of Forestry and Wildlife Management, Amherst, MA.

Castro-Santos, T. (2005). Optimal swim speeds for traversing velocity barriers: an analysis of volitional high-speed swimming behavior of migratory fishes. *The Journal of Experimental Biology, 208*, 421-432. doi:10.1242/jeb.01380

Chanson, H. (1999). Physical modelling of hydraulics. In *The Hydraulics of Open Channel Flow.* London, UK: Arnold.

Faber, D. M., Ploskey, G. R., Weiland, M. A., Deng, D., Hughes, J. S., Kim, J., . . . Skalski, J. R. (2011). *Evaluation of behavioral guidance structure on juvenile salmonid passage and survival at Bonneville Dam in 2009.* Richland, WA: Pacific Northwest National Laboratory.

Hall, C. J., Jordaan, A., & Frisk, M. G. (2012). Centuries of anadromous forage fish loss: consequences for ecosystem connectivity and productivity. *BioScience, 62*(8), 723-731. doi:10.1525/bio.2012.62.8.5

Hanson, B. (1999). Effectiveness of two surface bypass facilities on the Connecticut River to pass emigrating Atlantic salmon smolts. In *Innovations in fish passage technology.* Bethesda, Maryland: American Fisheries Society.

Haro, A., Odeh, M., Noreika, J., & Castro-Santos, J. (1998). Effect of water acceleration on downstream migratory behavior and passage of Atlantic salmon juvenile salmonids and

juvenile American shad at surface bypasses. *Transactions of the American Fisheries Society, 127*, 118-127.

Johnson, G. E., & Dauble, D. D. (2006). Surface flow outlets to protect juvenile salmonids passing through hydropower dams. *Reviews in Fisheries Science, 14*, 213-244.

Johnson, G. E., Adams, N. S., Johnson, R. L., Rondorf, D. W., Dauble, D. D., & Barila, T. Y. (2000). Evaluation of the prototype surface bypass for salmonid juvenile salmonids in spring 1996 and 1997 at Lower Granite Dam on the Snake River, Washington. *Transactions of the American Fisheries Society, 129*, 381-397.

Johnson, G. E., Anglea, S. M., Adams, N. S., & Wik, T. O. (2005). Evaluation of the prototype surface flow bypass for juvenile salmon and steelhead at the powerhouse of Lower Granite Dam, Snake River, Washington, 1996-2000. *North American Journal of Fisheries Management, 25*, 138-151.

Johnson, G. E., Giorgi, A. E., & Erho, M. W. (1997). *Critical assessment of surface flow bypass development in the lower Columbia and Snake rivers.* Completion Report for the U.S. Army Corps of Engineers, Portland and Walla Walla Districts.

Kemp, P. S., Gessel, M. H., & Williams, J. G. (2005). Fine-scale behavior responses of pacific salmonid smolts as they encounter divergence and accleration of flow. *Transactions of the American Fisheries Society, 134*(2), 390-398.

Kock, T. J., Liedtke, T. L., Ekstrom, B. K., Tomka, R. G., & Rondorf, D. W. (2012). *Behavior and passage of juvenile salmonids during the evaluation of a behavioral guidance structure at Cowlitz Falls Dam, Washington, 2011.* U.S. Geological Survey Open-File Report 2012-1030.

Larinier, M. (1998). Upstream and downstream fish passage experience in France, In: Fish Migration and Fish Bypasses. 127-145. (M. Jungwirth, S. Schmutz, & S. Weiss, Eds.) Blackwell Science Ltd Publisher.

Limburg, K. E., & Waldman, J. R. (2009). Dramatic declines in North Atlantic diadromous fishes. *BioScience, 59*(11), 955-965. doi:10.1525/bio.2009.59.11.7

Lundstrom, T. S., Gunnar, J., Hellstrom, I., & Lindmark, E. M. (2010). Flow design of guiding device for downstream fish migration. *River Research and Applications, 26*, 166-182.

McDowall, R. M. (1987). Evolution and importance of diadromy. *American Fisheries Society Symposium, 1*, 1-13.

NextEra Energy Maine Operating Services, LLC. (2010). *NextEra Energy diadromous fish passage report for the Lower Kennebec River watershed during the 2009 migration season.* Hallowell, ME.

Rakowski, C. L., Richmond, M. C., Serkowski, J. A., & Johnson, G. E. (2006). *Forebay computational fluid dynamics modeling for the Dalles Dam to support behavior guidance system siting studies.* Final Report. Prepared for the U.S. Army Corps of Engineers Portland District, Portland, Oregon Under a Related Services Agreement with the U.S. Department of Energy Contract DE-AC06-76RL01830.

Scott, S. (2012). A postive barrier fish guidance system designed to improve safe downstream passage of anadromous fish. *9th ISE 2012.* Vienna.

Tacoma Pubilic Utilities. (2010). *Cowlitz Falls behavioral guidance structure evaluation, Cowlitz River, Washington.* Prepared by HDR, Inc., Project No. 137396.

Taft, E. P. (2000). Fish protection technologies: a status report. *Environmental Science Policy, 3,* 5349-5359.

TransCanada Hydro Northeast Inc. (2012). *Bellow Falls Hydroelectric Project, FERC Project No. 1855.* Pre-application Document.

Venditti, D., Rondorf, D., & Kraut, J. (2000). Migratory behavior and forebay delay of radio-tagged juvenile fall chinook salmon in the lower Snake River impoundment. *North American Journal of Fisheries Management, 20,* 41-52.

Whitney, R., Calvin, L., Erho, M., & Coutant, C. (1997). *Downstream passage for salmon at hydroelectric projects in the Columbia River basin: development, installation, and evaluation.* Portland, OR: Northwest Power Planning Council.

Chapter 2: A physical modelling approach to evaluating the flow field upstream of a floating, impermeable guidance structure

1. Abstract

Impermeable guidance structures (or guide walls) are used to improve passage efficiency of out-migrating anadromous fish species. Their purpose is to guide the fish to a bypass (i.e. a sluice gate, weir, or pipe) allowing the fish to circumvent the turbine intakes and safely pass downstream. This paper details a series of experiments (nine total) performed at the USGS Conte Anadromous Fish Research Center located in Turners Falls, MA. The goal of the analysis was to measure the velocity components (x, y, and z) immediately upstream of the guide wall under a wide range of guide wall depths and angles to flow for a specified flow rate typical of a power canal. Two metrics are reported, the velocity magnitude and the Z-Velocity Ratio. These metrics are considered indicators of guidance difficulty and attempt to determine whether or not a fish will 1) encounter swim speeds greater than that of the fish is capable, 2) follow a negative rheotactic behavior and swim below the guide wall, and/or 3) be entrained by the downward flow and pass below the guide wall. Results indicate that a structure set at a small angle and deep enough such that the ineffective guidance zone at the lower section of the guide wall will be below the majority of approaching fish will perform the best.

2. Introduction

Guidance technologies such as louvers, impermeable guidance structures (or guide walls), and screens are prescribed to improve downstream fish passage at a hydroelectric facility (Schilt, 2007). They are intended to either induce behaviorally or actively guide the fish to a safer passage route (i.e. the bypass) and protect the fish from entering into the turbine intakes. The target species for these structures include a wide range of anadromous fish species, from bottom to surface oriented. The aim of this paper is to investigate the flow field upstream of a guidance wall, primarily intended to guide surface-oriented fish species such as salmonids and clupeids.

Guide walls were first introduced in 1995 at the Bellows Falls Dam on the Connecticut River in Vermont, USA and have been gaining popularity in the past 20 years, particularly in the northwestern United States (Mulligan et al. 2014). These structures introduce a strong downstream current in the direction of the bypass (Odeh, 1998) and offer full exclusion for fish swimming above the bottom of the wall. However, several studies have shown that there is a high propensity for fish to be temporarily guided along the structure only to then go underneath the guide wall into the direction of the turbine intakes (NextEra Energy Maine Operating Services, LLC, 2010; Kock et al., 2012; Faber et al., 2011). The fish may either be exhibiting negative rheotactic behavior (actively swimming in the same direction as the flow field), fatigued to the point of entrainment after attempting to swim against the downward flow field, be physically unable to swim against the encountered velocities, or responding to some other stimuli (i.e. turbulence, hydraulic strain, velocity gradients).

Mulligan et al. (2014) investigated the key design parameters of a guide wall (angle to approach flow, depth, and average approach velocity) through the use of a computational fluid dynamics (CFD) model in ANSYS Fluent V. 14.5. The key findings indicated that a guide wall set at a narrow angle (the minimum angle tested in the study was 25 degrees) and deep enough to maintain a low and relatively constant downward flow component in the range of the vertical distribution of the approaching fish species will perform the best. In this paper, the authors compare the findings from a lab scale physical model with those of Mulligan et al. (2014) and further detail the flow field immediately upstream of a guide wall.

The following series of experiments was conducted at the USGS Conte Anadromous Fish Research Center located in Turners Falls, MA with the financial support of the Hydro Research Foundation.

3. Experimental Design

The experiments were performed in a rectangular channel (hereafter referred to as the flume), 3 feet wide, 4 feet deep, and 16.25 feet long, with a plywood floor and acrylic sides. The flume was attached to a head and tail tank, which received and released the flow (Fig. 1). The head tank received the flow of water through a 10" pipe connected to a pump which raised the water from a sump below the laboratory room floor into the head tank. A calibrated 12" Venturi meter was attached to the 10" pipeline immediately upstream of where the water entered into the head tank. The high and low pressure lines of the Venturi meter were attached to piezometers. The differential head was used to calculate the flow into the head tank and subsequently the flume. The pipe line into the head tank was perpendicularly oriented to the head tank floor. At the base of the pipe, two 6" wide by 6" high slits regulated the water flow into the head tank. Each opening forced the water to go in the direction of the upstream head tank wall. A total of 3 screens placed perpendicular to the head tank floor were used to diffuse the flow into the flume,

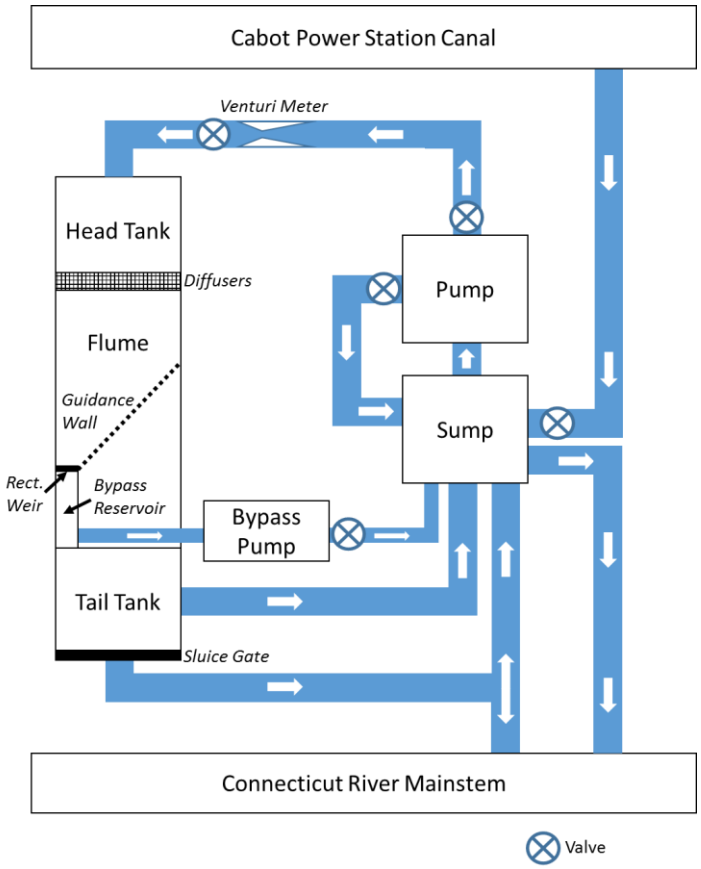

Figure 1: A schematic of the laboratory, showing all water diversions.

removing a significant portion of the entrained air and creating a more uniform flow distribution at the entrance. There were two outlets in the tail tank, the majority of flow went through a circular opening in the wall on the downstream side of the tail tank. The flume was allowed to fully drain through a low flow outlet which was a circular opening on the tail tank floor. The outlet on the wall face had an adjustable sluice gate attached which allowed the modelers to adjust the water elevation in the flume. The water that flowed out the opening on the wall face was partially recycled back into the sump, whereas the other portion (exact percent unknown) drained back out to the Connecticut River main stem. The entire flow was not recycled back into the sump due to structural limitations. The water which flowed out the low flow outlet fully drained back into the sump. The water elevation in the sump was maintained via a gravity-driven line from the Cabot Station power canal, immediately northeast of the laboratory.

Within the flume, a guidance wall was constructed of a series of ¾" double-sided MDO plywood panels. The guidance wall was fixed in place on the upstream end to a wooden piece attached to the flume wall via a clamp and on the downstream end to the bypass reservoir via a hinge fixed onto the bypass reservoir wall. The hinge allowed the modelers to easily change the angle of the guide wall, after removing a section of the plywood. The way this was constructed led to minor differences in the velocity distribution at the start of the guidance wall (discussed further in the Experimental Results Section) because the start location of the guide wall within the flume varied depending upon the angle. The hinge was attached such that it could be shifted up and down to change the depth of the guide wall. The bypass reservoir was constructed of ¾" double-sided MDO plywood and the existing plywood floor and acrylic sides of the flume. The reservoir was 3" wide, 30" high, and 34.5" long. Water flowed into the bypass reservoir via a sharp-crested rectangular weir made of aluminum. The weir was set in place such that it could be shifted up and down to change the amount of flow into the weir. Water exited the bypass reservoir via a 3"circular outlet near the base of the reservoir. A 5 horsepower pump was used to extract the water from the reservoir. Flow measurements into the bypass reservoir were made using the rectangular weir equation (Crowe et al., 2005). The coefficient of discharge was estimated using the Rehbock Equation (Rehbock, 1929), which takes into account the depth of the water upstream of the weir and the height of the weir.

The lab model is a scaled down version (1:20) of an idealized guidance wall configuration set in a rectangular power channel, referred to as the prototype. Fig. 2 shows the model schematic. Note the x-y-z axis orientation for later reference. Emphasis is placed on the lab version to display similarity in form (geometric similarity), motion (kinematic similarity), and forces (dynamic similarity) to the prototype, as recommended by Chanson (1999). The primary force ratios considered are the Froude number (a ratio of the inertial force to the gravitational force) and the Reynolds number (a ratio of the inertial force to the viscous force). The lab version and the prototype possess identical Froude numbers, although vary significantly in Reynolds number. Acknowledging this limitation, the goal becomes to ensure that turbulent flow ($Re > 10^4$) exists

in all lab model versions. It is important to note that 1) it is impossible to match both Froude and Reynolds numbers for a prototype and laboratory model, 2) Froude similarity provides the best results for models where friction effects are negligible, and 3) significantly greater velocities in the laboratory model are required to match the prototype Reynolds number making it infeasible to perform in the laboratory setting of this study (Heller, 2011). Table 1 details each lab model configuration and the associated prototype model. Other pertinent parameter values that are fixed include W (channel width: 30 in. -- laboratory, 50 ft. -- prototype), H (water depth: 30 in., 50 ft.), w (rectangular weir width: 3 in., 5 ft.), b (head of water above rectangular weir: 3.6 in., 6 ft.), Q_T (total flow rate into flume: 2.8 cfs, 5000 cfs), Q_B (total flow rate into the bypass reservoir: 0.14 cfs, 250 cfs), and Q_C (total flow rate under guide wall: 2.66 cfs, 4750 cfs). The Reynolds number for each experiment at the start of the guidance wall is approximately 2.65×10^4, for the prototype the value is approximately 2.37×10^6. The flow for both the prototype and laboratory experiments is subcritical ($Fr = 2.88 \times 10^{-2}$).

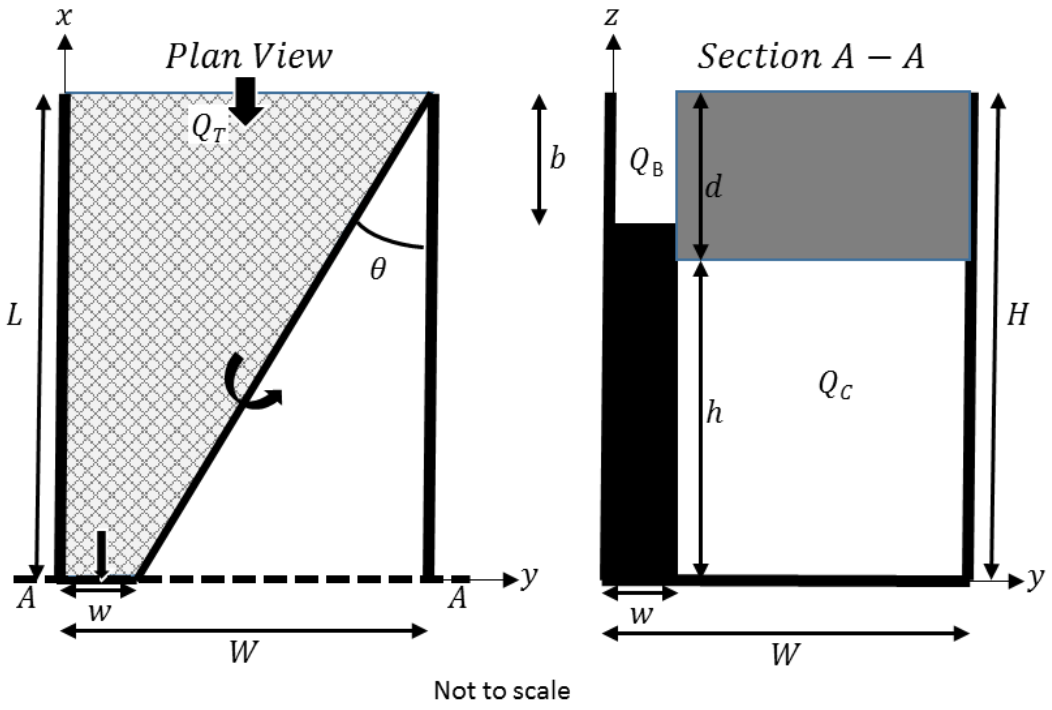

Figure 2: The laboratory model schematic. Plan view is shown on the left, the hatched area represents the region where data was collected. L is the longitudinal length of the model, which measures the distance along the x-axis between the bypass weir (x = 0) and the start of the guidance wall (x = L). This changes depending upon the angle of the structure, θ.

Table 2: Parameter values of each experiment, comparing the laboratory version to the prototype. V is the calculated average approach velocity given the flow rate of the experiment and the water depth. The L subscript refers to the laboratory version and the P subscript refers to the prototype. All other parameters in the table were previously defined.

Experiment #	θ	Q_B/Q_T	Laboratory Version		Prototype	
			V_L (fps)	d_L (in.)	V_P (fps)	d_P (ft.)
1	15	0.05	0.4	6	2	10
2	15	0.05	0.4	8	2	13.33
3	15	0.05	0.4	10	2	16.67
4	30	0.05	0.4	6	2	10
5	30	0.05	0.4	8	2	13.33
6	30	0.05	0.4	10	2	16.67
7	45	0.05	0.4	6	2	10
8	45	0.05	0.4	8	2	13.33
9	45	0.05	0.4	10	2	16.67

4. Experimental Results

To quantitatively evaluate the flow field, a SonTek Acoustic Doppler Velocimeter (ADV) was used to measure the velocity components in 3 dimensions. This ADV can measure flow velocities far less than 1 mm/s to over 2.5 m/s and acquires data at a sampling rate of 25 Hz. The sampling volume of the ADV is approximately 1.9" below the tip of the probe. A grid was set up in the region upstream of the guide wall (see the hatched area of Fig. 2) and contour plots of the flow field were constructed using this data assuming a linear change between points. The grid was unevenly spaced, with tighter spacing closer to the FIGS and the water surface. Number of data points for each experiment ranged from 101 to 183, largely reflective of the angle to flow of the configuration. Data was taken at cross-sections at multiple locations along the guide wall, including immediately upstream of the start of the guide wall and immediately upstream of the bypass rectangular weir. In total 6 cross-sections were taken for Experiments 1-3, 5 for Experiments 4-6, and 4 for Experiments 7-9. The probe collected data at a duration of 60 seconds per data point, which at a sampling rate of 25 Hz amounts to 1500 measurements per data point. Other time durations were tested (30s, 90s), but it was determined that 60s was adequate to obtain accurate and reliable velocity measurements.

As illustrated in Mulligan et al. (2014), the strong downward flow component that exists along guidance walls can negatively affect the guidance efficiency of these structures. The authors also proposed the idea of an effective guidance depth for these structures, recognizing the fact that a lower section of the guide wall is less likely to guide fish to the bypass as a result of the higher downward velocity component in this region. Fig. 3 is a photo taken of the midway section of the guidance wall for Experiment 6, where red dye was released directly onto the guidance wall at multiple depths in the water column. It clearly shows the varying degree in the downward flow component from each of these locations, becoming greater the deeper into the water column. Considering this important and problematic feature of a guide wall, metrics are developed which seek to explore whether a fish will 1) follow a negative rheotactic approach and swim downward below the guide wall and 2) be entrained by the velocity field and forced underneath the guide wall (whether by fatigue or not having the physical capability of swimming fast enough to oppose the flow).

Figure 3: A photo taken of red dye released onto the guide wall of Experiment 6 at different depths. Red arrows are superimposed over the image to show the direction of the water. The top of the guide wall is immediately above the top arrow.

As a consequence of the method used to build the guide wall, the starting point varies for the experiments of different angles. This results in differing velocity distributions at x = L (the upstream starting point of the guide wall). Fig. 4 shows a contour plot of the mean of the velocity magnitude measurements (mean taken over the 1500 samples per data point) collected at x = L. The flow regime of each experiment shows some similarities, with the highest velocities occurring in the center of the flume, and the lowest along the walls. However, the maximum velocity magnitude does differ for each experiment, decreasing as the angle is increased and the start of the guide wall moves further downstream. This downstream movement allows for a more uniform flow distribution to be obtained.

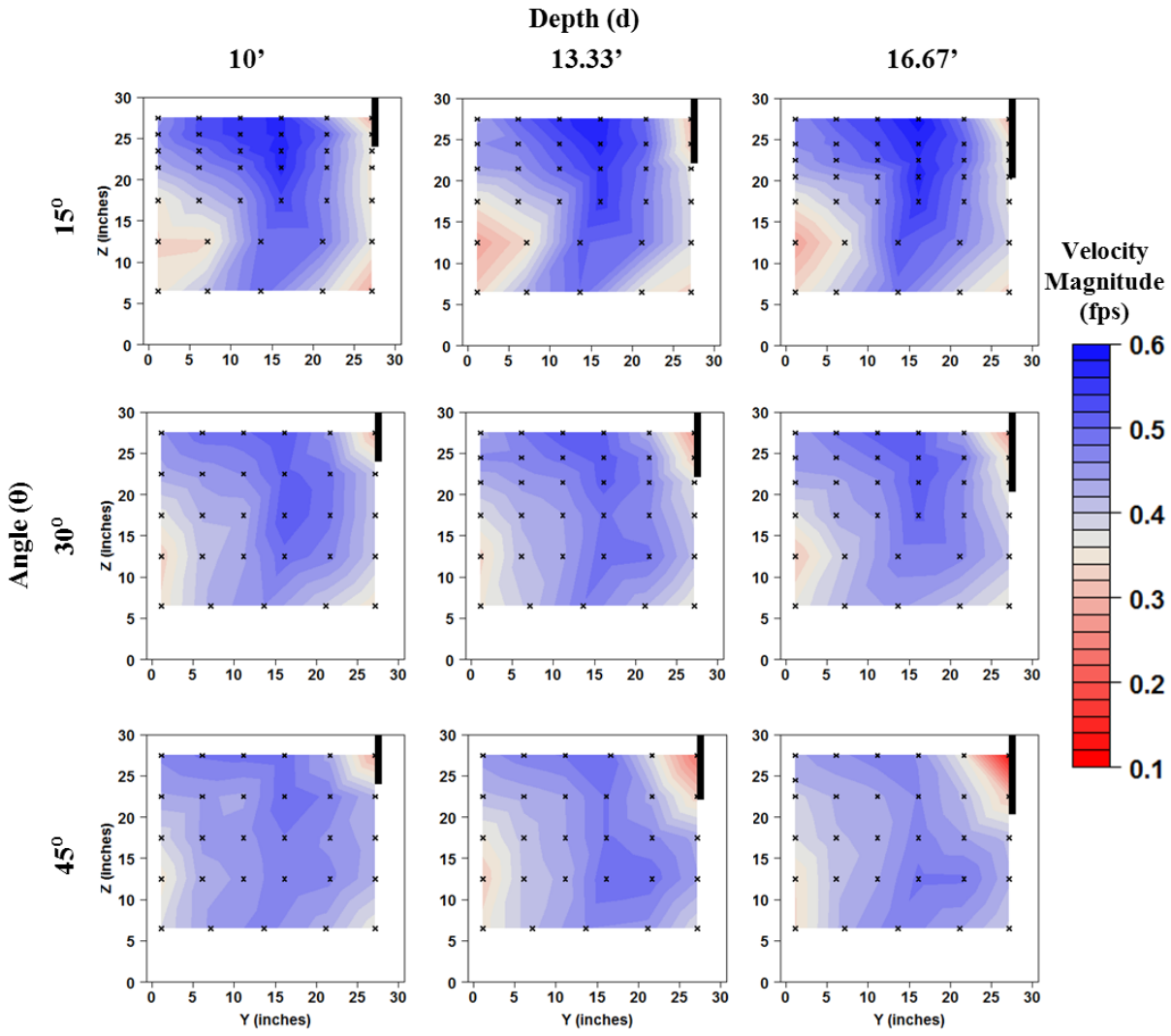

Figure 4: Contour plots of the mean velocity (mean taken over the 1500 samples per data point) for each experiment. The black x-marks indicate the location of the data point. The black rectangle indicates the location of the guide wall. The contour plots are for the location of x = L.

The differences in velocity at the start of the guide wall carries through and impacts the velocity magnitude throughout the model domain. Fig. 5 displays the mean (left) and maximum (right) velocity magnitude above the bottom of the guide wall for each experiment at x = L (top) and x = .29L to .38L (bottom). The average velocity in the region above the bottom of the guide wall at x = L varies from 0.42 fps to 0.5 fps for all the experiments, with the maximum occurring for Experiment 1. The mean velocity is shown to change only slightly between the two locations, unlike the maximum velocity magnitude which is sensitive to a change in the depth and/or angle of the structure. At x = .29L to .38L, Experiment 9 has a mean velocity magnitude of 0.42 fps and a maximum of 0.62 fps, nearly a 50% difference. At this same location Experiment 1 has a mean velocity magnitude of 0.5 fps and a maximum velocity of 0.54 fps, a difference of only 8%. Fig. 6 shows this maximum to mean velocity magnitude ratio at the location of x = .29L to .38L, truly highlighting the impact of the guide wall configuration.

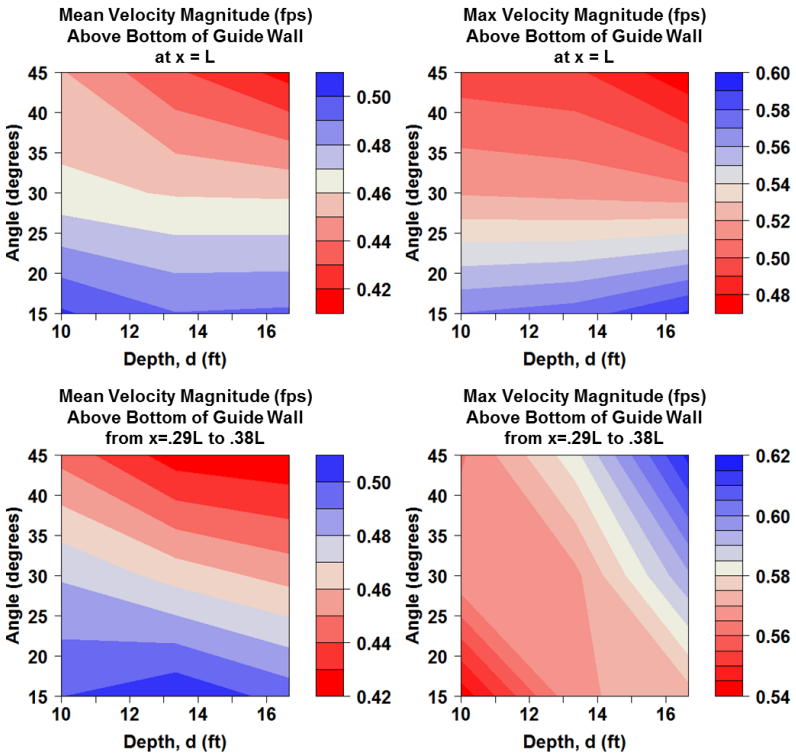

Figure 5: Mean (left column) and maximum (right column) velocity magnitude above the bottom of the guide wall for each experiment at x = L (top row) and x = .29L to .38L (bottom row).

It should be noted before continuing that the average velocity at x = L varies only from 0.43 fps to 0.45 fps within the data collection area of the cross-sections (see the colored region of the cross-sections shown in Fig. 4). For the given flow rate, Q_T, and the height of the water column, H, it was expected to have an average velocity across the entire cross-section of the flume equal to 0.4 fps. The averages for each cross-section would shift closer to 0.4 fps if data for the entire cross-section of the flume was collected. The regions outside the data collection area of each cross-section would have lower velocities due to wall friction effects.

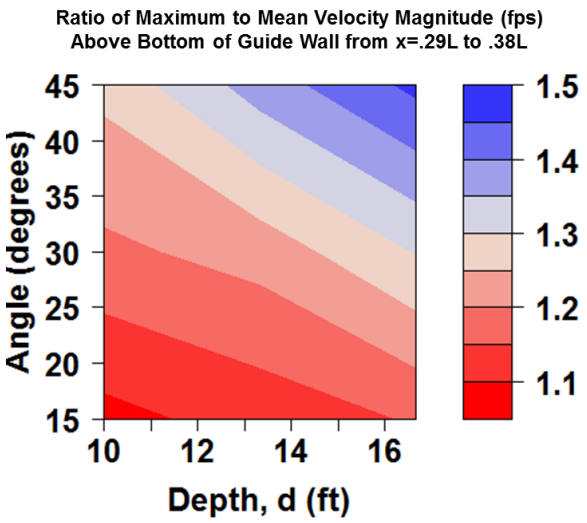

Figure 6: Maximum to mean velocity magnitude ratio at the location of x = .29L to .38L

The supplemental material section shows plots of the velocity magnitude at all cross-sections where data was collected. In it there appears evidence that a pocket of slower moving water develops beside the guide wall in the top portion of the water column as the water around it accelerates downward acting as a partial barrier to movement, slowing the water down. This pocket grows as the angle and depth are increased resulting in a large velocity gradient in the z-direction beside the guide wall. This velocity gradient becomes greater as the angle and depth are increased.

Overall, the velocities shown around these structures for an average approach velocity of approximately 2 fps in prototype terms likely isn't high enough to pose physical swimming capability problems to most adult out-migrating fish species. They may however be susceptible to fatigue as these structures can be particularly long. There is a clear tradeoff in decreasing the angle to 15 degrees as this will achieve lower peak velocities but will also increase the length in which the fish must be capable of swimming along the structure. Less is certain about juvenile swim speed capability, but it is generally understood that they will be more easily entrained in the flow field. Ideally juvenile fish will be able to drift downstream and use their limited swimming capability to be safely guided to the bypass. We will use the following metric to address whether or not a fish (juvenile or adult) will be more or less likely to be entrained below the guide wall or follow a negative rheotactic behavior and actively swim below the guide wall.

The second metric highlighted in this paper is the Z-Velocity Ratio, or the ratio of the velocity in the z-direction to the magnitude of the x and y velocity components. Here the authors' assume that the larger the magnitude of the Z-Velocity Ratio along the guide wall, the more likely a fish

will be to exhibit a negative rheotactic behavior or be entrained below the guide wall. The Z-Velocity Ratio at each data point is calculated using the following formula:

$$\frac{\bar{V}_z}{\sqrt{\bar{V}_x^2+\bar{V}_y^2}} \qquad \text{Eq. (1)}$$

Where $\bar{V}_z$ is the mean velocity in the z-direction taken over the 60 second data collection period for each data point, $\bar{V}_x$is the mean velocity in the x-direction, and $\bar{V}_y$is the mean velocity in the y-direction. Fig. 7-15 displays Z-Velocity Ratio contour plots of each cross-section where data was collected for each experiment. A negative value indicates a downward flow, away from the water surface.

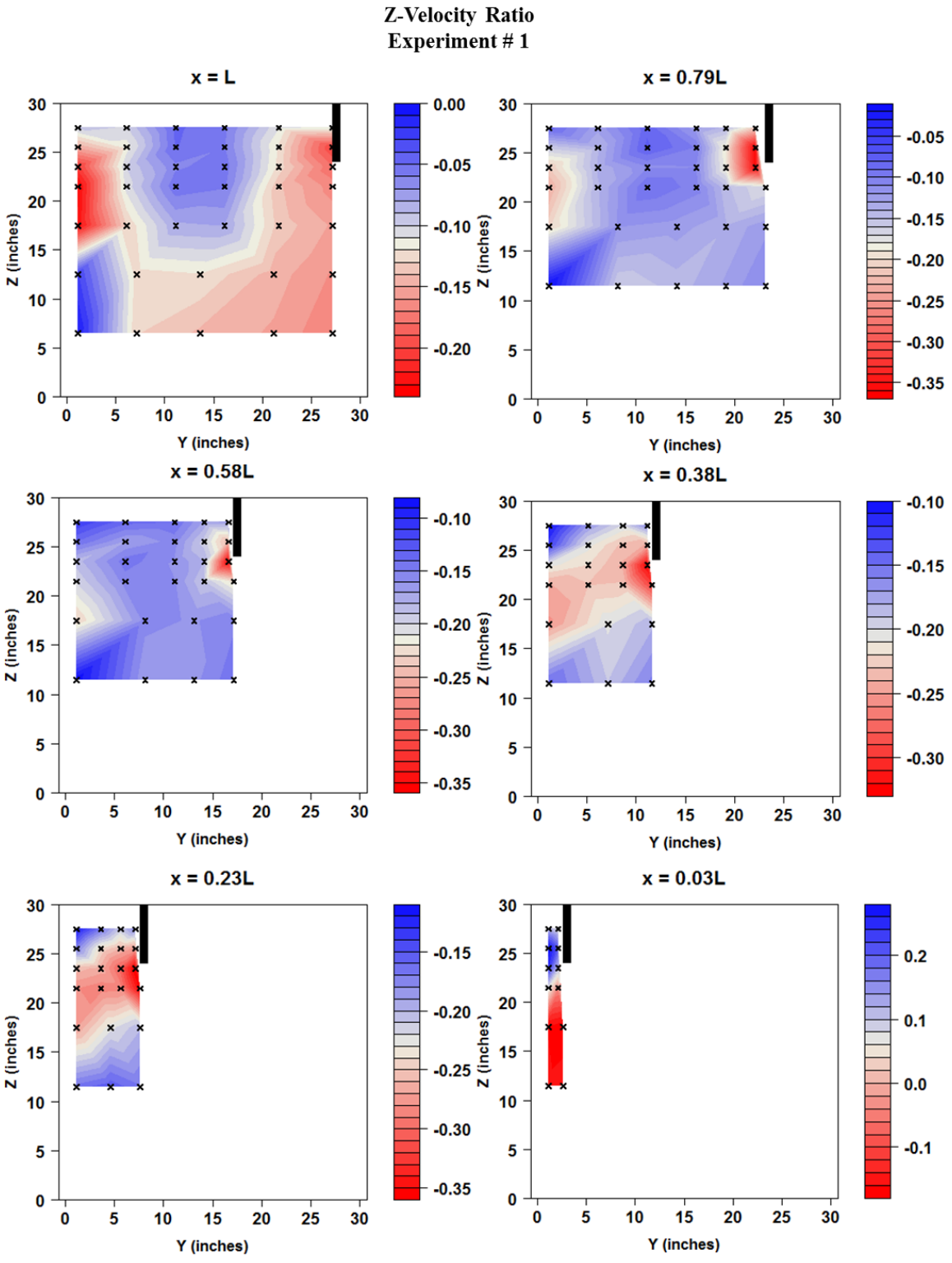

Figure 7: Z-Velocity Ratio for Experiment 1. The black "x's" indicate the location of each data point. Values were interpolated between each data point assuming a linear relationship. The black rectangle indicates the location of the guide wall in relation to the cross-section.

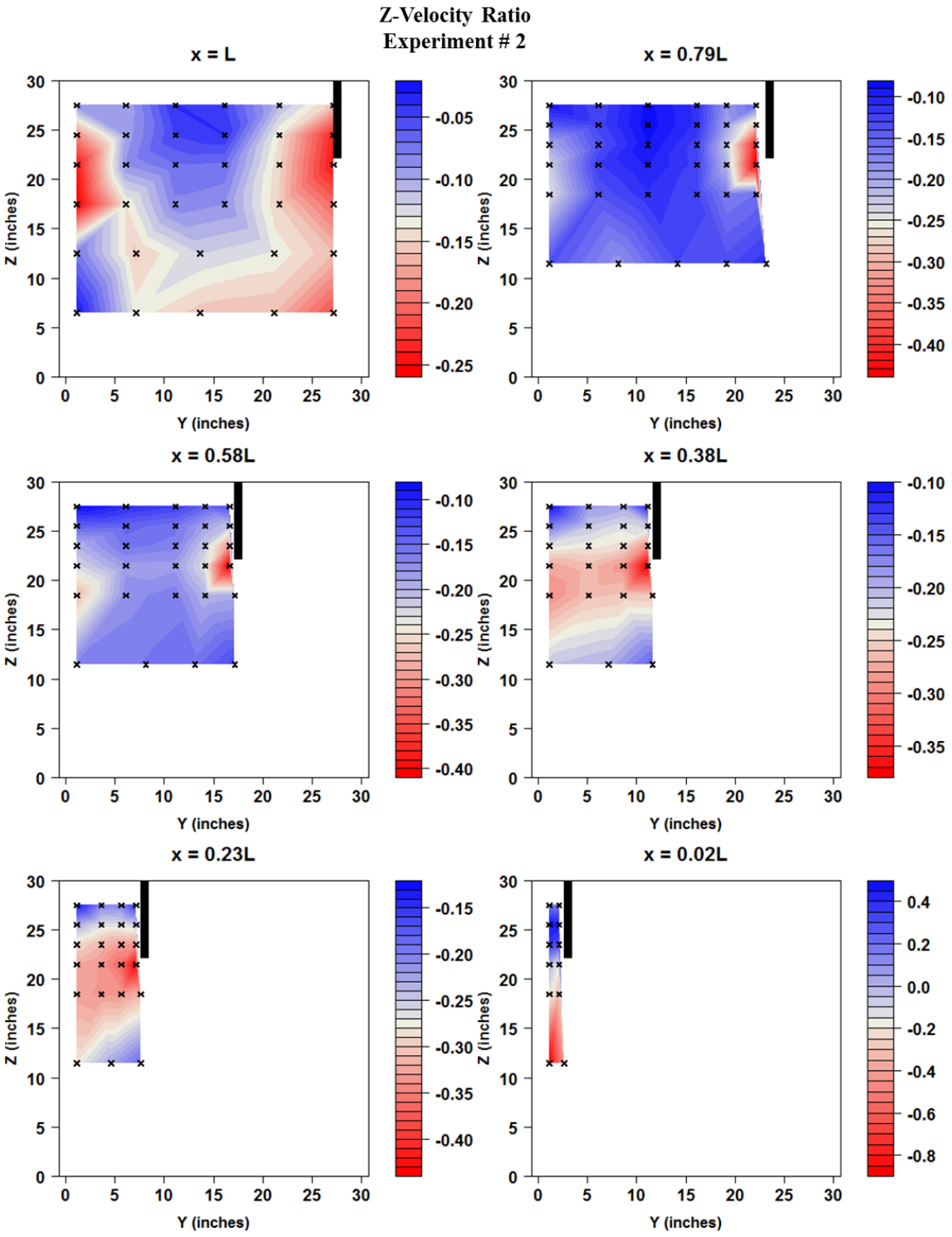

Figure 8: Z-Velocity Ratio for Experiment 2. The black "x's" indicate the location of each data point. Values were interpolated between each data point assuming a linear relationship. The black rectangle indicates the location of the guide wall in relation to the cross-section.

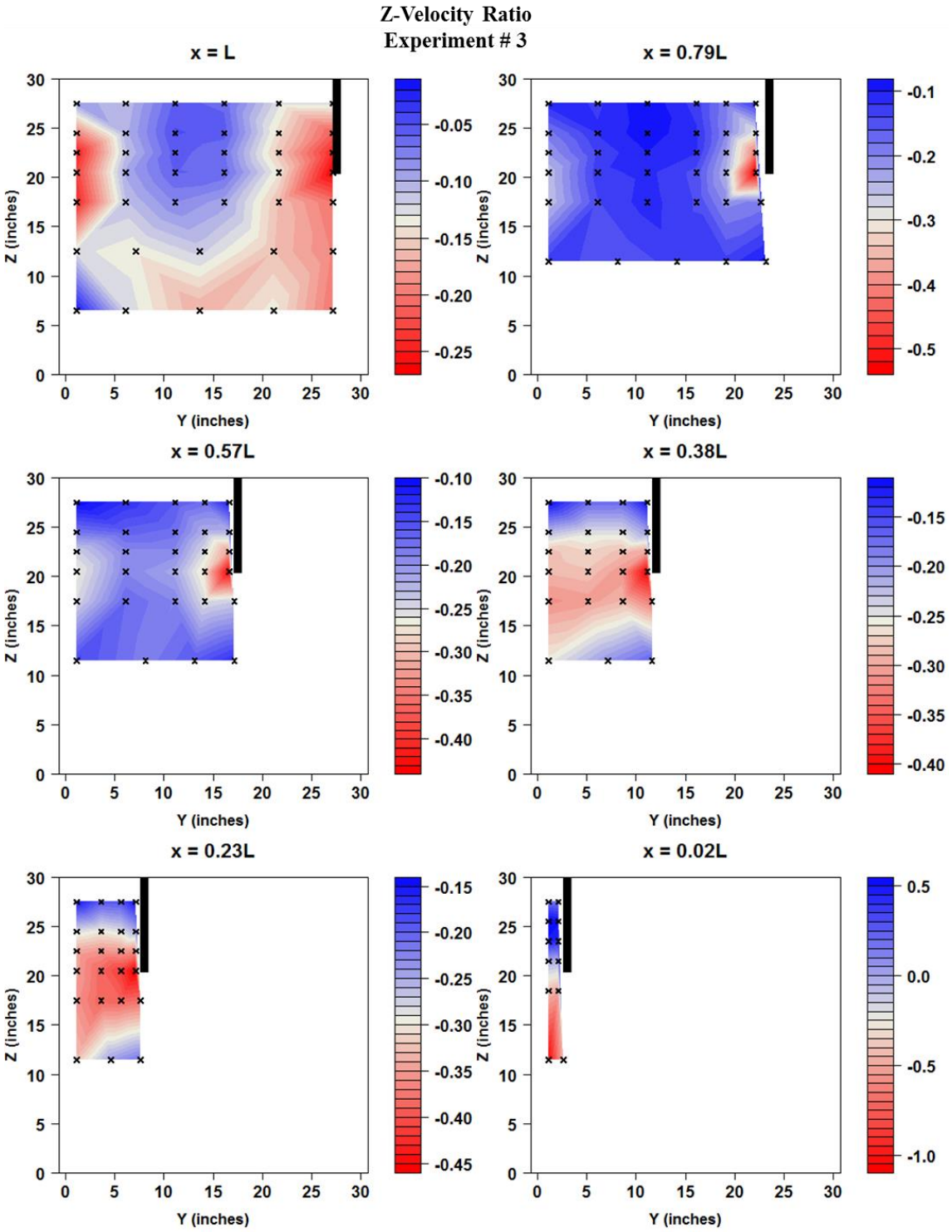

Figure 9: Z-Velocity Ratio for Experiment 3. The black "x's" indicate the location of each data point. Values were interpolated between each data point assuming a linear relationship. The black rectangle indicates the location of the guide wall in relation to the cross-section.

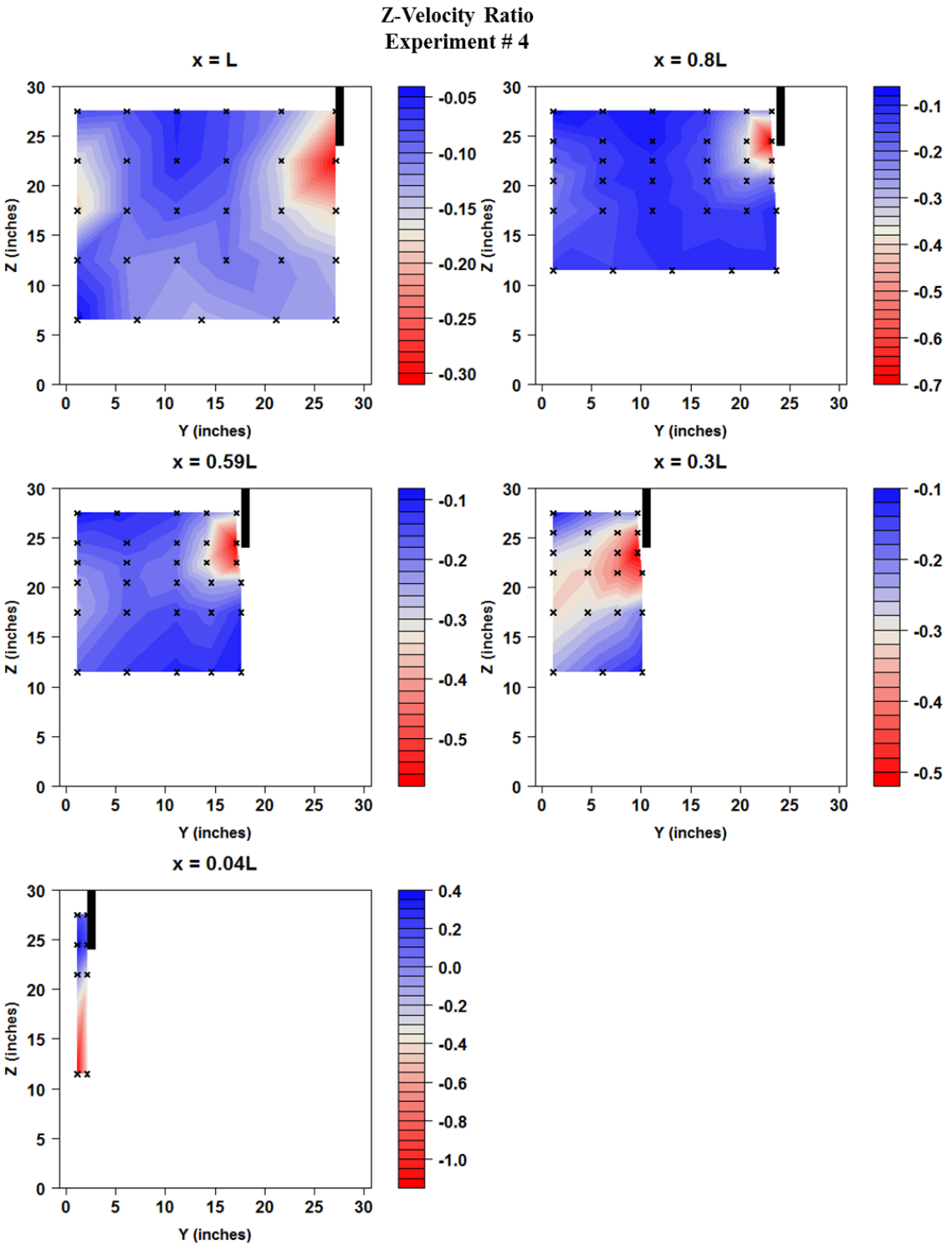

Figure 10: Z-Velocity Ratio for Experiment 4. The black "x's" indicate the location of each data point. Values were interpolated between each data point assuming a linear relationship. The black rectangle indicates the location of the guide wall in relation to the cross-section.

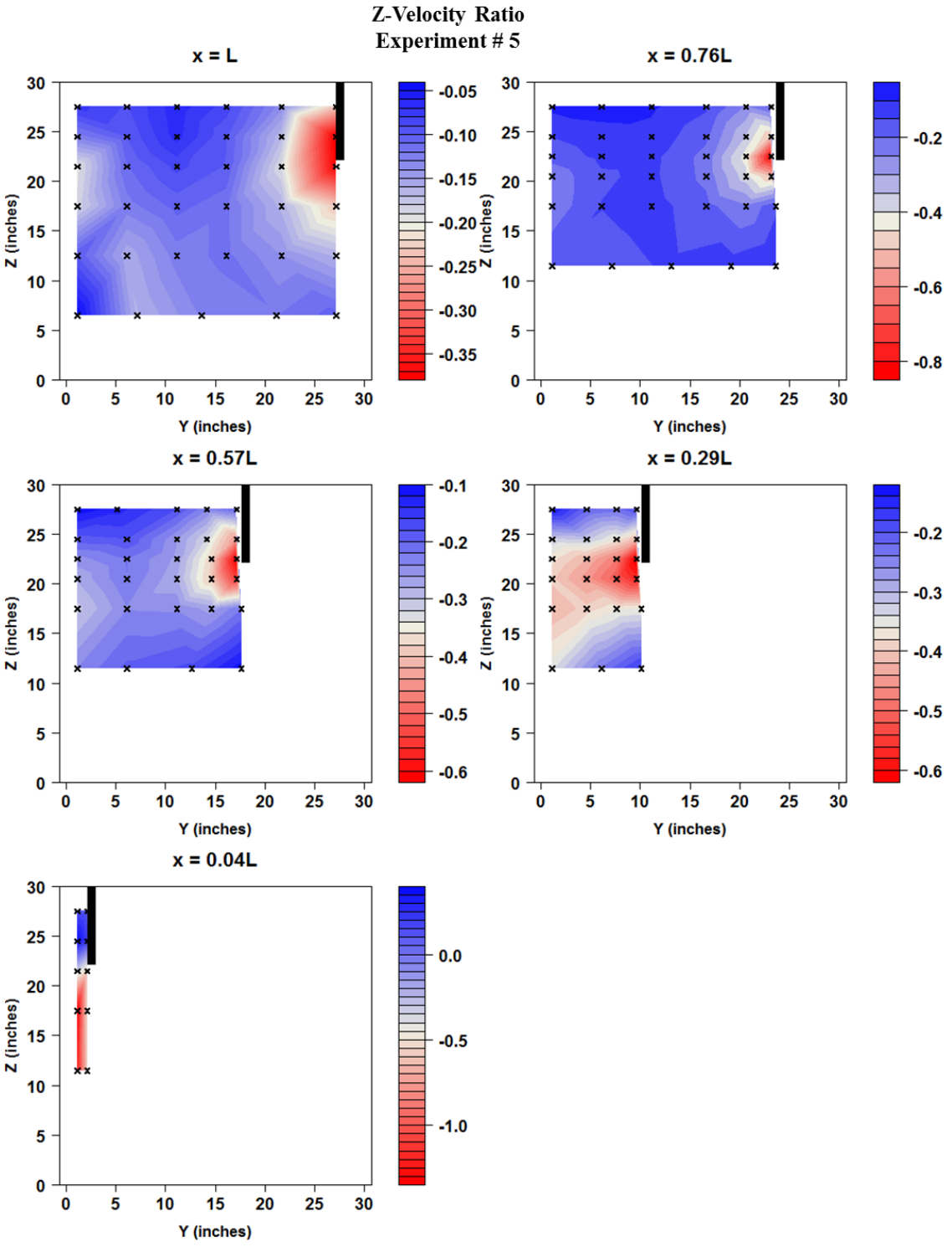

Figure 11: Z-Velocity Ratio for Experiment 5. The black "x's" indicate the location of each data point. Values were interpolated between each data point assuming a linear relationship. The black rectangle indicates the location of the guide wall in relation to the cross-section.

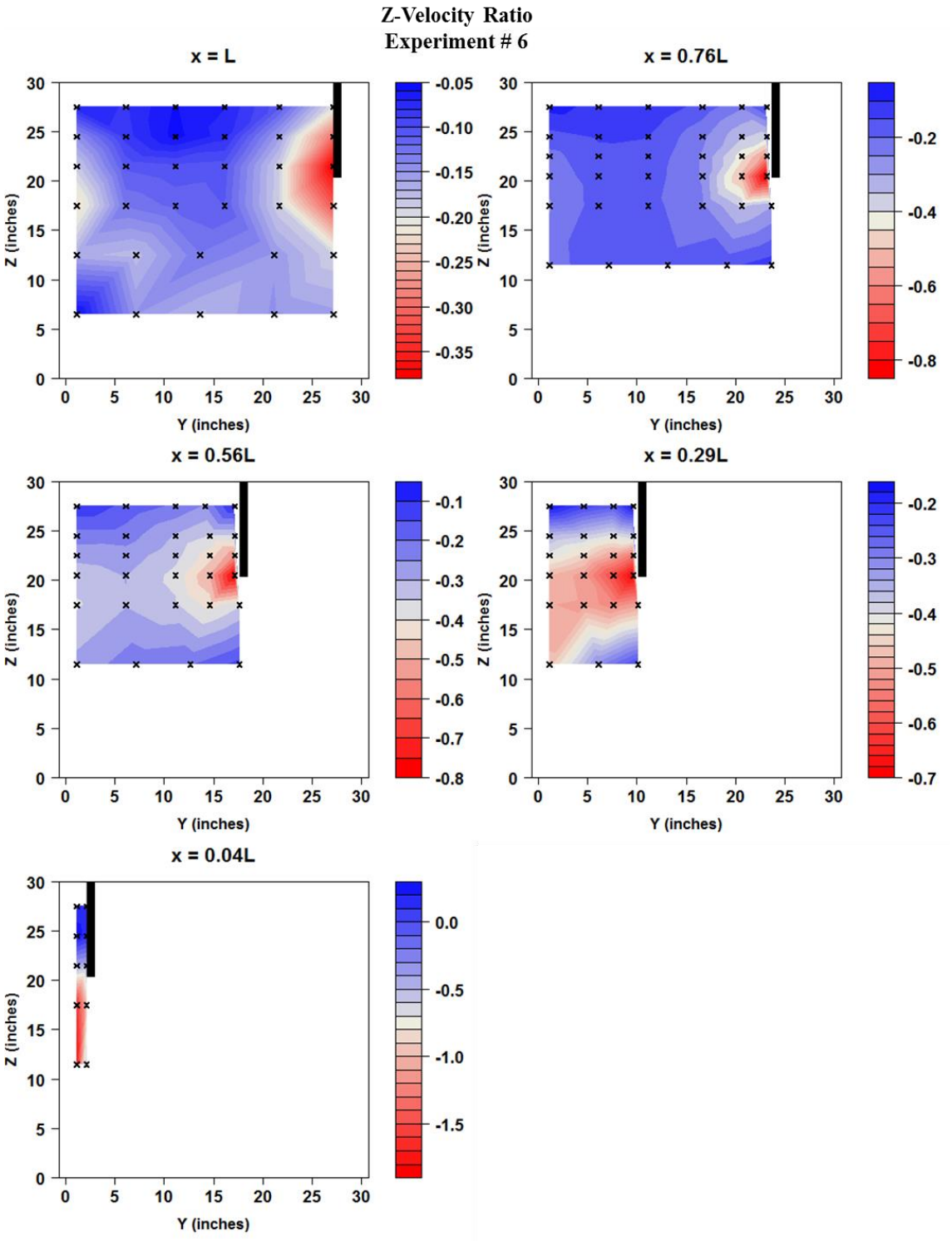

Figure 12: Z-Velocity Ratio for Experiment 6. The black "x's" indicate the location of each data point. Values were interpolated between each data point assuming a linear relationship. The black rectangle indicates the location of the guide wall in relation to the cross-section.

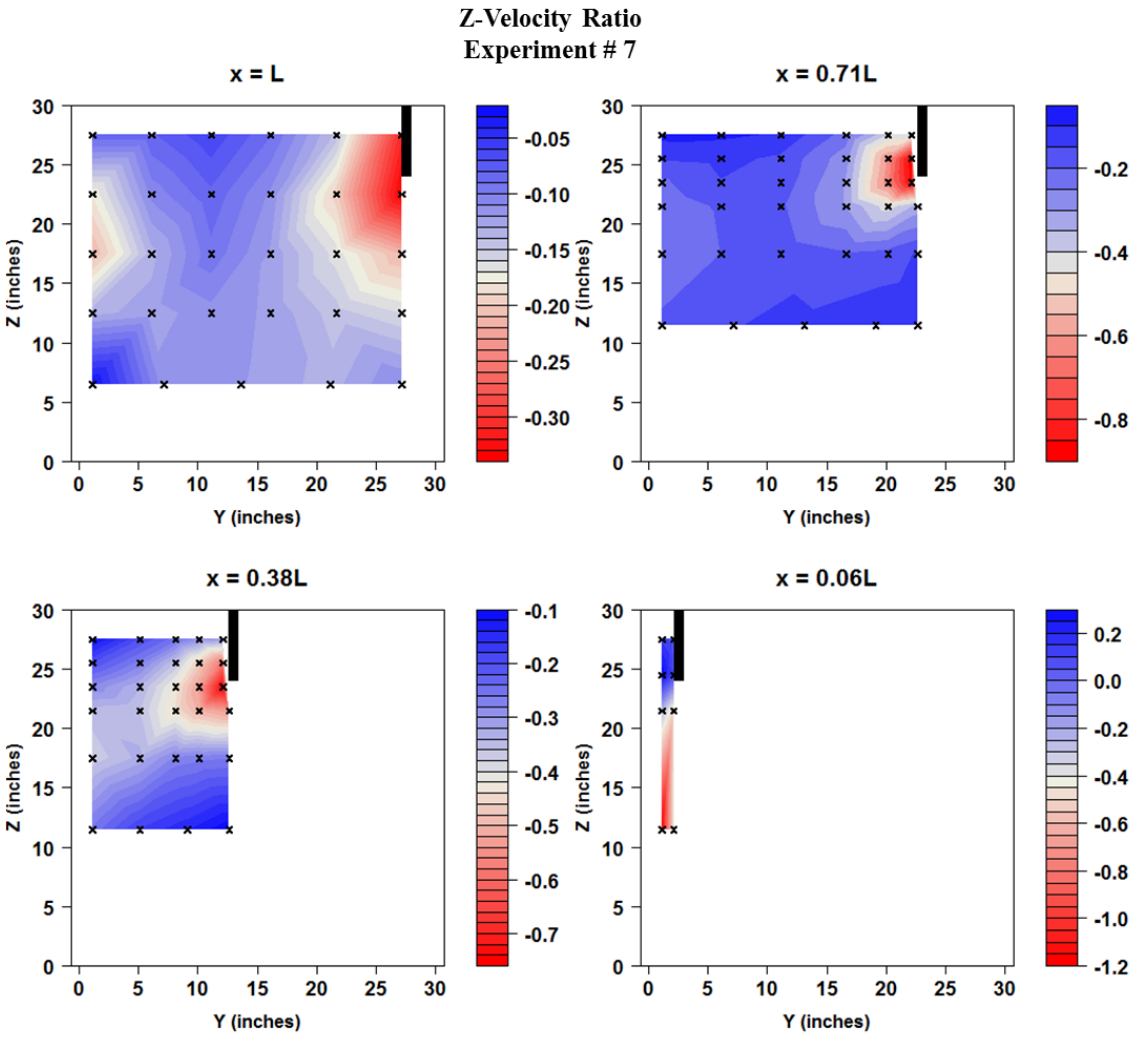

Figure 13: Z-Velocity Ratio for Experiment 7. The black "x's" indicate the location of each data point. Values were interpolated between each data point assuming a linear relationship. The black rectangle indicates the location of the guide wall in relation to the cross-section.

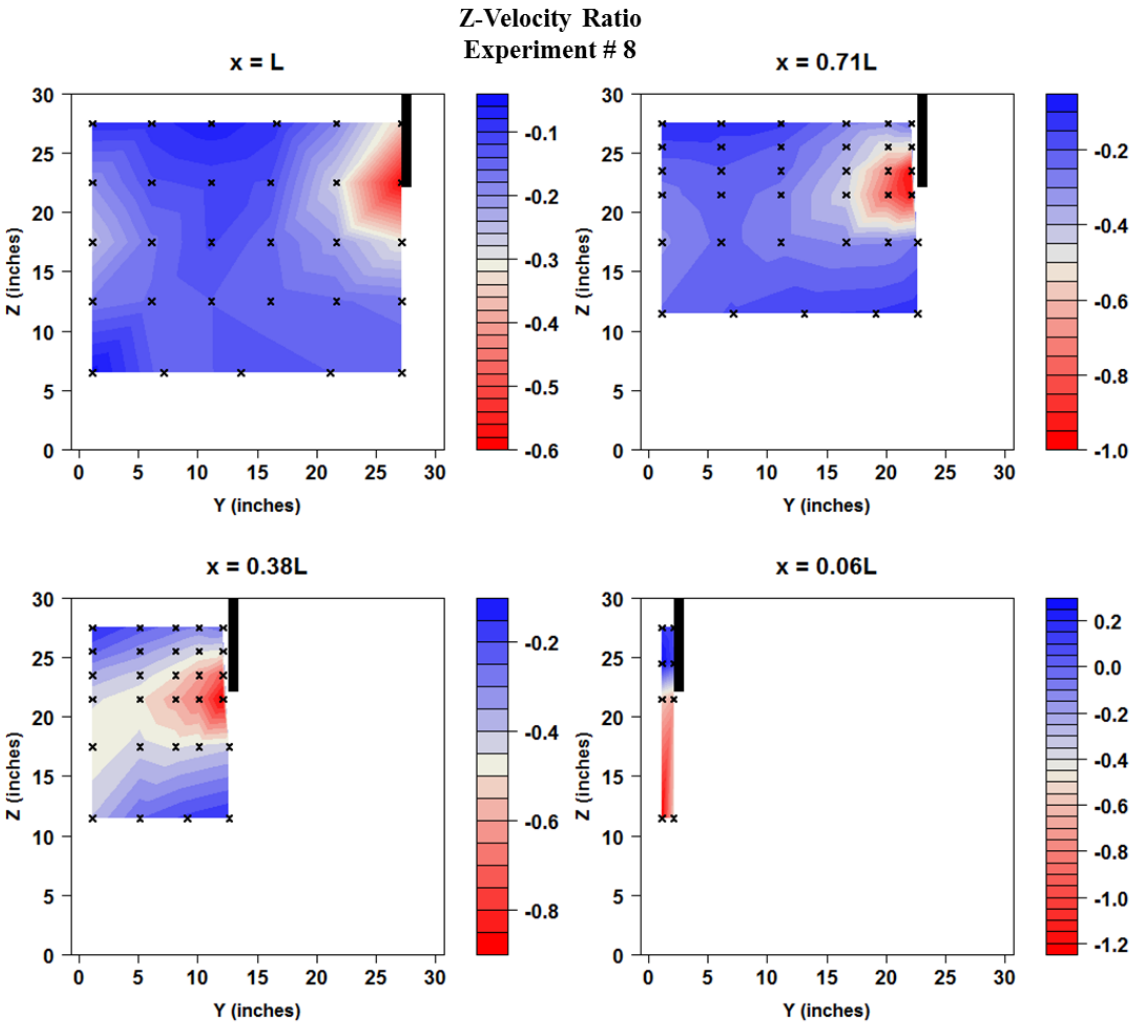

Figure 14: Z-Velocity Ratio for Experiment 8. The black "x's" indicate the location of each data point. Values were interpolated between each data point assuming a linear relationship. The black rectangle indicates the location of the guide wall in relation to the cross-section.

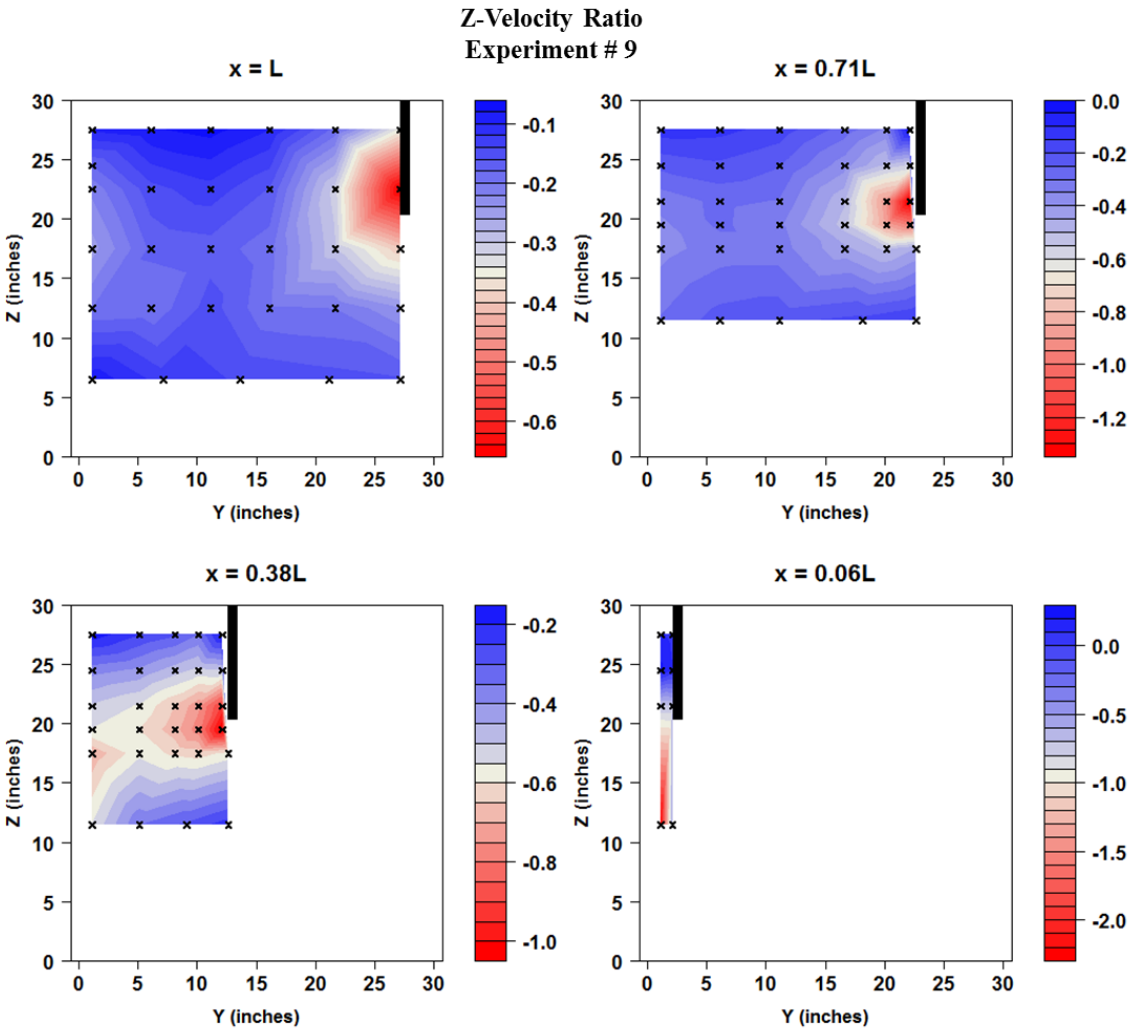

Figure 15: Z-Velocity Ratio for Experiment 9. The black "x's" indicate the location of each data point. Values were interpolated between each data point assuming a linear relationship. The black rectangle indicates the location of the guide wall in relation to the cross-section.

Fig. 7-15 demonstrates the effect of a guide wall on the Z-Velocity Ratio. In general, negative Z-Velocity Ratio's exist throughout the data set, except for directly in front of the bypass weir. The magnitude of the metric increases both when the depth of the guide wall is increased and the angle to flow is increased. The minimum Z-Velocity Ratio occurs directly beside the very bottom of the guide wall. Fig. 16 displays a contour plot of the minimum Z-Velocity Ratio for each experiment where x is between 0.71L and 0.8L. The Z-Velocity Ratio is slightly greater at this location than further downstream. It clearly shows the sensitivity of this value to both the depth and angle of the structure. A 45 degree guide wall set at the deepest depth of 16 2/3' (in prototype terms) results in the peak negative value of -1.35, whereas a 15 degree guide wall set at the shallowest depth of 10' results in a Z-Velocity Ratio of only -.4.

Furthermore, a large gradient of the Z-Velocity Ratio in the z-direction forms directly beside the guide wall. For instance, Experiment 9 shows that a fish located near the mid-section of the guide wall at x = .38L would experience a Z-Velocity Ratio of about -0.2 when swimming in the top 5 feet (in prototype terms) of the water column directly along the guide wall, but would experience a Z-Velocity Ratio of approximately -1.0 when traveling along the very bottom of the guide wall, between 15 and 20 feet deep. That change is dramatic and, along with the peak velocity magnitudes occurring at the bottom of the guide wall, supports the notion that these structures are ineffective at guiding fish to a bypass when traveling at a depth near the bottom of the guide wall.

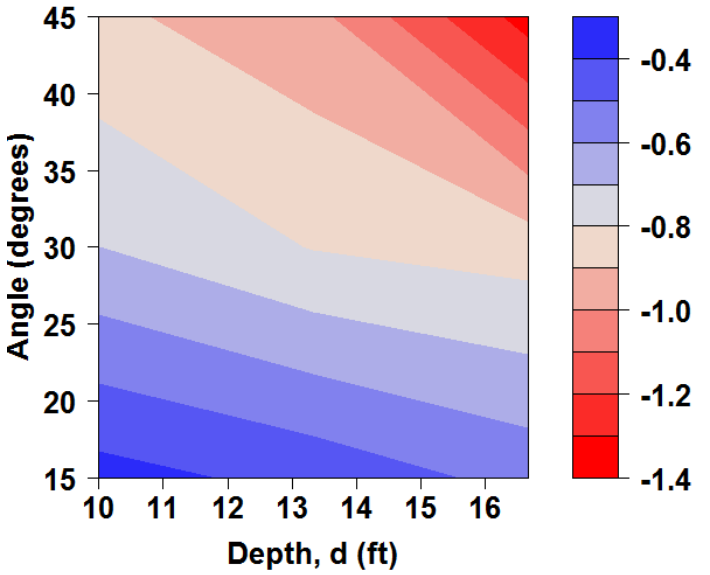

Figure 16: Contour plot of the minimum Z-Velocity Ratio for each experiment where x is between 0.71L and 0.8L.

To expand on this point, Table 2 shows a postulated effective guidance depth (EGD) for each experiment determined by finding the location along the face of the guide wall where the Z-Velocity Ratio goes above (in magnitude terms) a threshold value, shown in the table to vary between -0.1 and -1.4. The cells colored light blue indicate that the EGD for the specified threshold is equal to the depth of the structure. The red colored cells indicate that the EGD is equal to or less than the depth of the uppermost data point taken at each cross-section, a depth in prototype terms of roughly 4.2'.

Table 3: Postulated effective guidance depth (EGD) for each experiment in relation to a threshold Z-Velocity Ratio.

		Depth, d_p (ft)	Angle, θ (deg.)	Threshold Z-Velocity Ratio													
				-0.1	-0.2	-0.3	-0.4	-0.5	-0.6	-0.7	-0.8	-0.9	-1	-1.1	-1.2	-1.3	-1.4
Experiment	1	10.0	15	≤ 4.2	≤ 4.2	6.2	10.0	10.0	10.0	10.0	10.0	10.0	10.0	10.0	10.0	10.0	10.0
	2	13.3	15	≤ 4.2	5.3	7.9	10.6	13.3	13.3	13.3	13.3	13.3	13.3	13.3	13.3	13.3	13.3
	3	16.7	15	≤ 4.2	4.5	9.4	12.3	15.0	16.7	16.7	16.7	16.7	16.7	16.7	16.7	16.7	16.7
	4	10.0	30	≤ 4.2	≤ 4.2	4.6	5.7	6.9	8.0	10.0	10.0	10.0	10.0	10.0	10.0	10.0	10.0
	5	13.3	30	≤ 4.2	≤ 4.2	5.2	7.2	9.3	10.4	11.4	12.5	13.3	13.3	13.3	13.3	13.3	13.3
	6	16.7	30	≤ 4.2	≤ 4.2	6.5	9.7	11.4	12.9	14.1	15.4	16.7	16.7	16.7	16.7	16.7	16.7
	7	10.0	45	≤ 4.2	≤ 4.2	≤ 4.2	4.2	4.8	5.5	6.2	7.0	10.0	10.0	10.0	10.0	10.0	10.0
	8	13.3	45	≤ 4.2	≤ 4.2	≤ 4.2	5.8	7.5	8.3	9.0	9.7	10.4	13.3	13.3	13.3	13.3	13.3
	9	16.7	45	≤ 4.2	≤ 4.2	≤ 4.2	5.5	8.7	9.5	10.1	10.8	11.4	12.1	12.7	13.3	13.9	16.7

The postulated EGD builds upon the work of Mulligan et al. (2014). The authors developed a metric called the "Work Indicator" which had an identical aim and determined values for a complete range of depths along the guide wall. The advantage of the Work Indicator was that it took into account both the downward velocity of the water and the length of the path (and in doing so the length of the guide wall) using CFD model output. Here we take a different approach and characterize the EGD based solely on the Z-Velocity Ratio and thus focus our efforts on whether or not a fish will intentionally swim below the guide wall or be entrained underneath it, rather than considering the fatigue a fish may experience when attempting to oppose the flow. Table 2 shows that the postulated EGD, given a relatively low threshold value of -0.4, increases for a decrease in the angle of the structure. However, it is unclear what the threshold truly should be, particularly when it is likely to vary by species and age of the fish. But for the sake of discussion let's assume that a threshold value of -0.7 is a good measure of the propensity for fish to swim below the guide wall. Anything greater in magnitude than this threshold would result in the fish swimming or being entrained below the structure. Then we can clearly see from Table 2 that the only guide wall configurations that possess an EGD equal to the depth of the guide wall is Experiments 1-4. All other experiments have a potentially ineffective lower section of the guide wall ranging from 1.9 to 6.6' from the bottom of the wall. This is significant given the cost of these structures among other factors. A greater knowledge of how fish respond to this particular metric and the depth at which the fish approach the guide wall could lead to significant improvement regarding the analysis. The main takeaway from the Z-Velocity Ratio results is that structures set at angles greater than 15 degrees should be set considerably deeper than the expected swimming depth of the fish to accommodate for these potentially ineffective guidance zones.

5. Discussion & Conclusion

Over the past 20 years, impermeable guidance structures, or guide walls, have been utilized to increase the survivability of anadromous out-migrating fish while in the presence of a hydroelectric dam. The experiments performed in this study focused on the hydraulic impact of the key design parameters (angle and depth) of these structures while building upon the work of Mulligan et al. (2014). The key findings largely agree with the conclusions made in Mulligan at al. (2014), although there are some differences. We learned through studying the velocity magnitude that even in the case of Experiment 9 where the angle is 45 degrees and the depth is 16 2/3', the maximum velocity magnitude is roughly 50% larger than the average approach velocity. This increase, while potentially significant, likely does not pose a limitation to the physical swimming capability of most out-migrating adult fish species. This result is in direct conflict with that of Mulligan et al. (2014), where the study showed that for a similar configuration to Experiment 7 velocities could exceed 4 times the average approach velocity. The authors are currently revisiting this study to ensure model accuracy prior to submittal of their work to a journal for publishing.

We then showed that the maximum velocity magnitude and the minimum Z-Velocity Ratio occur at the bottom of the guide wall. The combination of these two peaks lead the authors to believe that, as Mulligan et al. (2014) proposed, a bottom section of the guide wall is potentially ineffective at guiding fish to the bypass. Even if an adult out-migrating fish can physically oppose the velocity magnitude it will be more likely to follow its negative rheotactic behavior and swim below the guide wall. As for juvenile fish, these large Z-Velocity Ratio's show that when just passively traveling with the flow field they will be at great risk of being entrained below the guide wall.

In consideration of these arguments, the author's recommend that a guide wall be set deep enough such that the deepest point of the expected vertical distribution of the fish will be less than or equal to the EGD. However, a better understanding of fish behavior in the presence of these structures is required to know the true threshold of the Z-Velocity Ratio in which we use to measure the EGD. Although we do believe that the most effective measure to increase the percentage of EGD to the depth of the structure is by decreasing the angle. Therefore a 15 degree structure should outperform a 30 or 45 degree structure of the same depth given the same vertical distribution of the approaching fish. Increasing the guide wall depth will increase the EGD (although as shown in Table 2 not as much as the increase in the guidance depth), but it results in higher peak velocities and a greater magnitude of the Z-Velocity Ratio in the ineffective region of the guide wall. Thus those fish traveling deeper than expected in the water column are to have a lesser chance at being safely guided to the bypass. Therefore, to offer a general rule, it is likely a better practice to reduce the angle of the structure when possible rather than increasing the depth (unless of course the majority of the approaching fish are deeper than the guide wall).

Future work is necessary, this includes 1) measuring the flow field under different approach velocities and different percent of flow to the bypass, 2) estimation of head loss and overall cost of the project, and 3) testing in situ with the various fish species of interest to better understand their behavioral response to the structure.

6. Acknowledgements

The information, data, or work presented herein was funded in part by the Office of Energy Efficiency and Renewable Energy (EERE), U.S. Department of Energy, under Award Number DE-EE0002668 and the Hydro Research Foundation.

The work was made possible by those at the USGS Conte Anadromous Fish Research Center located in Turners Falls, MA, including Barnaby Watten and John Noreika.

7. Disclaimer

their employees, makes and warranty, express or implied, or assumes and legal liability or responsibility for the accuracy, completeness, or usefulness of any information, apparatus, product, or process disclosed, or represents that its use would not infringe privately owned rights. Reference herein to any specific commercial product, process, or service by trade name, trademark, manufacturer, or otherwise does not necessarily constitute or imply its endorsement, recommendation or favoring by the United States Government or any agency thereof. The views and opinions of authors expressed herein do not necessarily state or reflect those of the United States Government or any agency thereof.

8. References

ANSYS Fluent, Release 14.5, Help System, ANSYS, Inc. (n.d.).

Chanson, H. (1999). Physical modelling of hydraulics. In *The Hydraulics of Open Channel Flow.* London, UK: Arnold.

Crowe, C. T., Elger, D. F., & Roberson, J. A. (2005). *Engineering Fluid Mechanics* (8th ed.). Hoboken, NJ: John Wiley & Sons, Inc.

Faber, D. M., Ploskey, G. R., Weiland, M. A., Deng, D., Hughes, J. S., Kim, J., . . . Skalski, J. R. (2011). *Evaluation of behavioral guidance structure on juvenile salmonid passage and survival at Bonneville Dam in 2009.* Richland, WA: Pacific Northwest National Laboratory.

Heller, V. (2011). Scale effects in physical hydraulic engineering models. *Journal of Hydraulic Research, 49*(3), 293-306. doi:10.1080/00221686.2011.578914

Kock, T. J., Liedtke, T. L., Ekstrom, B. K., Tomka, R. G., & Rondorf, D. W. (2012). *Behavior and passage of juvenile salmonids during the evaluation of a behavioral guidance structure at Cowlitz Falls Dam, Washington, 2011.* U.S. Geological Survey Open-File Report 2012-1030.

Mulligan, K. B., Towler, B., Haro, A., & Ahlfeld, D. (2014). A review of floating impermeable guidance structures and how their design parameters effect the flow field (to be submitted).

NextEra Energy Maine Operating Services, LLC. (2010). *NextEra Energy diadromous fish passage report for the Lower Kennebec River watershed during the 2009 migration season.* Hallowell, ME.

Odeh, M., & Orvis, C. (1998). Downstream fish passage design considerations and developments at hydroelectric projects in the Northeast USA. In M. Jungwirth, S. Schmutz, & S. Weiss (Eds.), *Fish Migration and Fish Bypasses* (pp. 267-280). Oxford, UK: Fishing New Books.

Rehbock, T. (1929). Wassermessung mit scharfkantigen Ueberfallwehren, Z. VDI. *73*(27), 817-823.

Schilt, C. R. (2007). Developing fish passage and protection at hydropower dams. *Applied Animal Behaviour Science, 104,* 295-325. doi:10.1016/j.applanim.2006.09.004

9. Supplemental Material

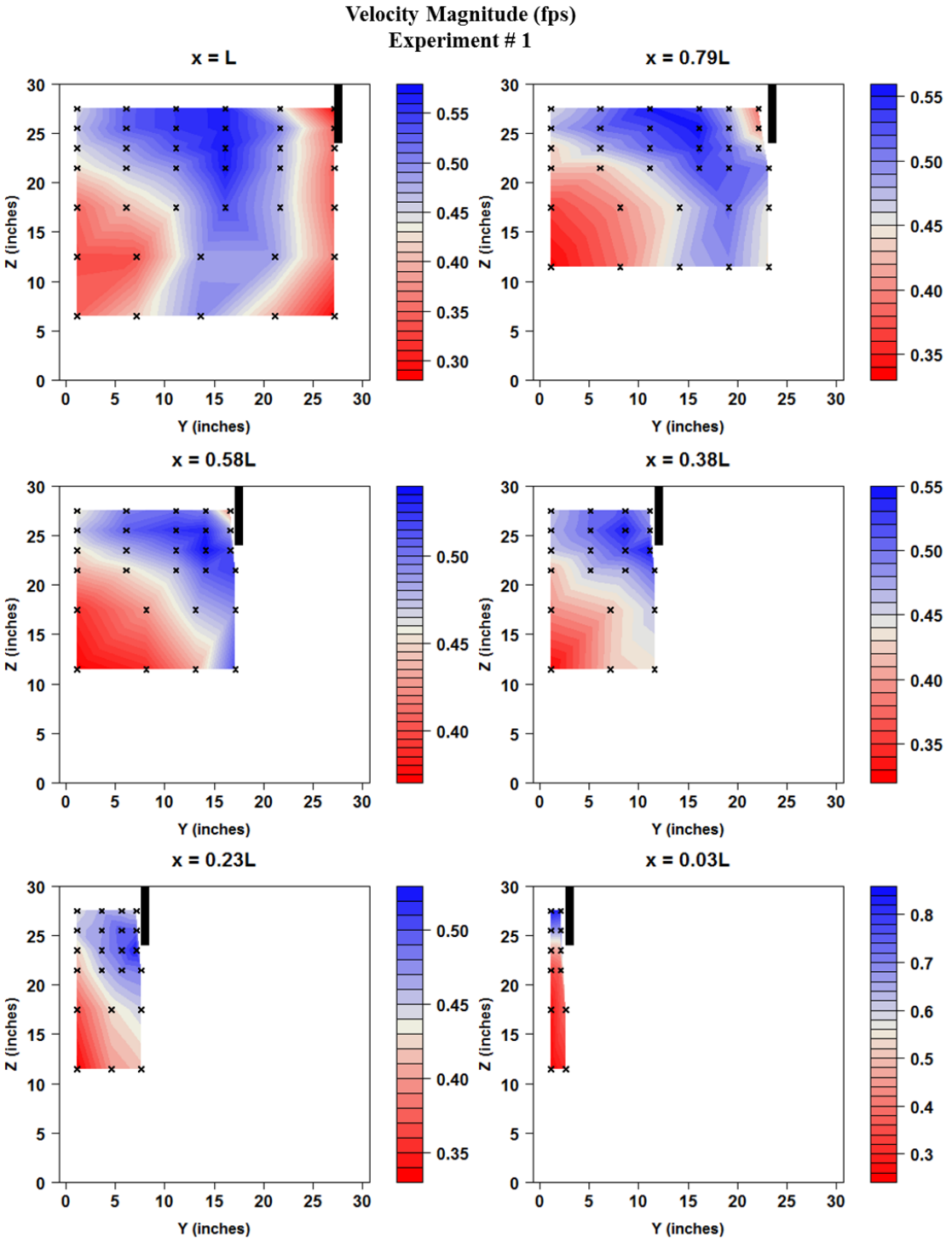

Figure 17: Velocity Magnitude for Experiment 1. The black "x's" indicate the location of each data point. Values were interpolated between each data point assuming a linear relationship. The black rectangle indicates the location of the guide wall in relation to the cross-section.

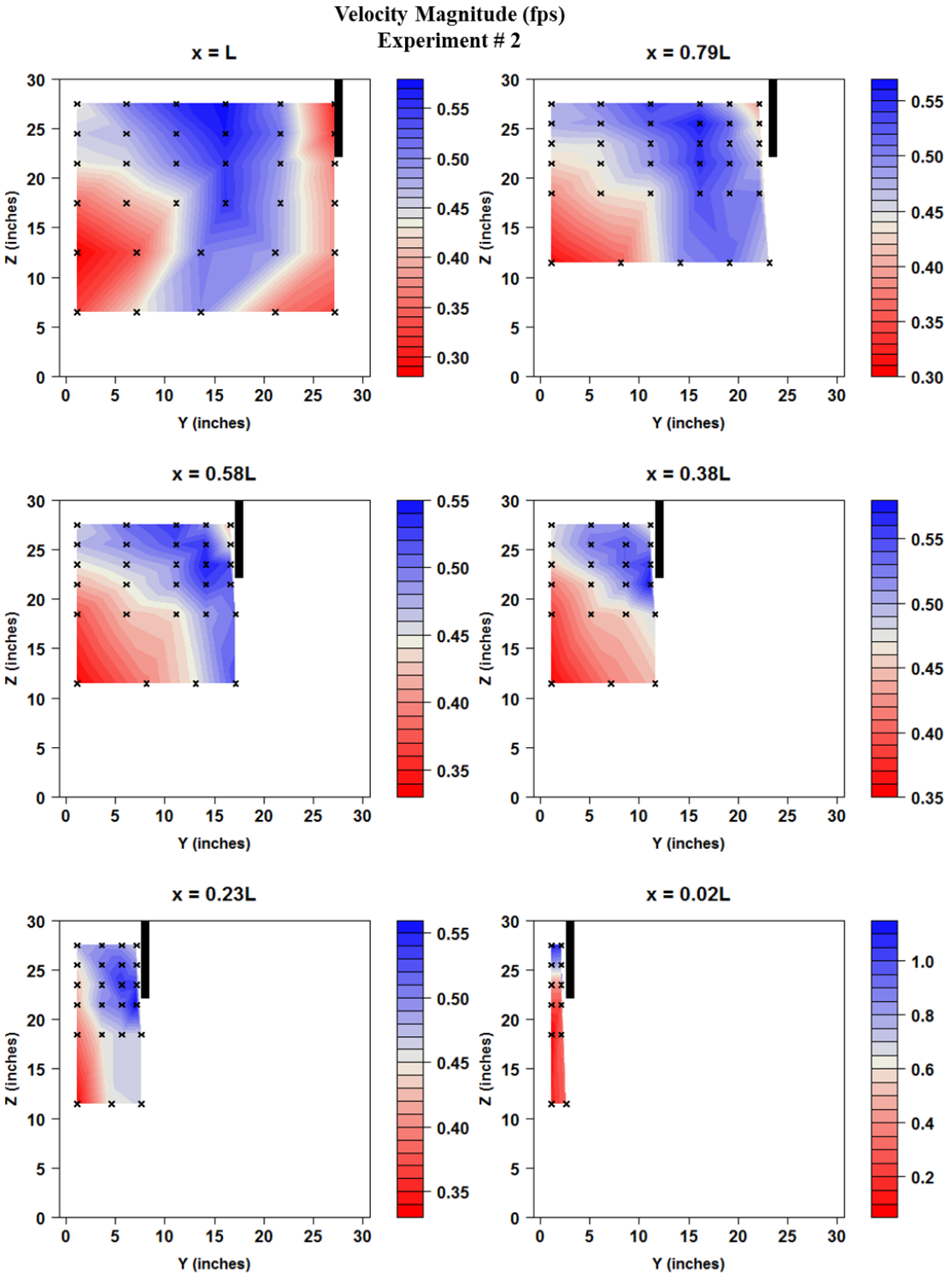

Figure 18: Velocity Magnitude for Experiment 2. The black "x's" indicate the location of each data point. Values were interpolated between each data point assuming a linear relationship. The black rectangle indicates the location of the guide wall in relation to the cross-section.

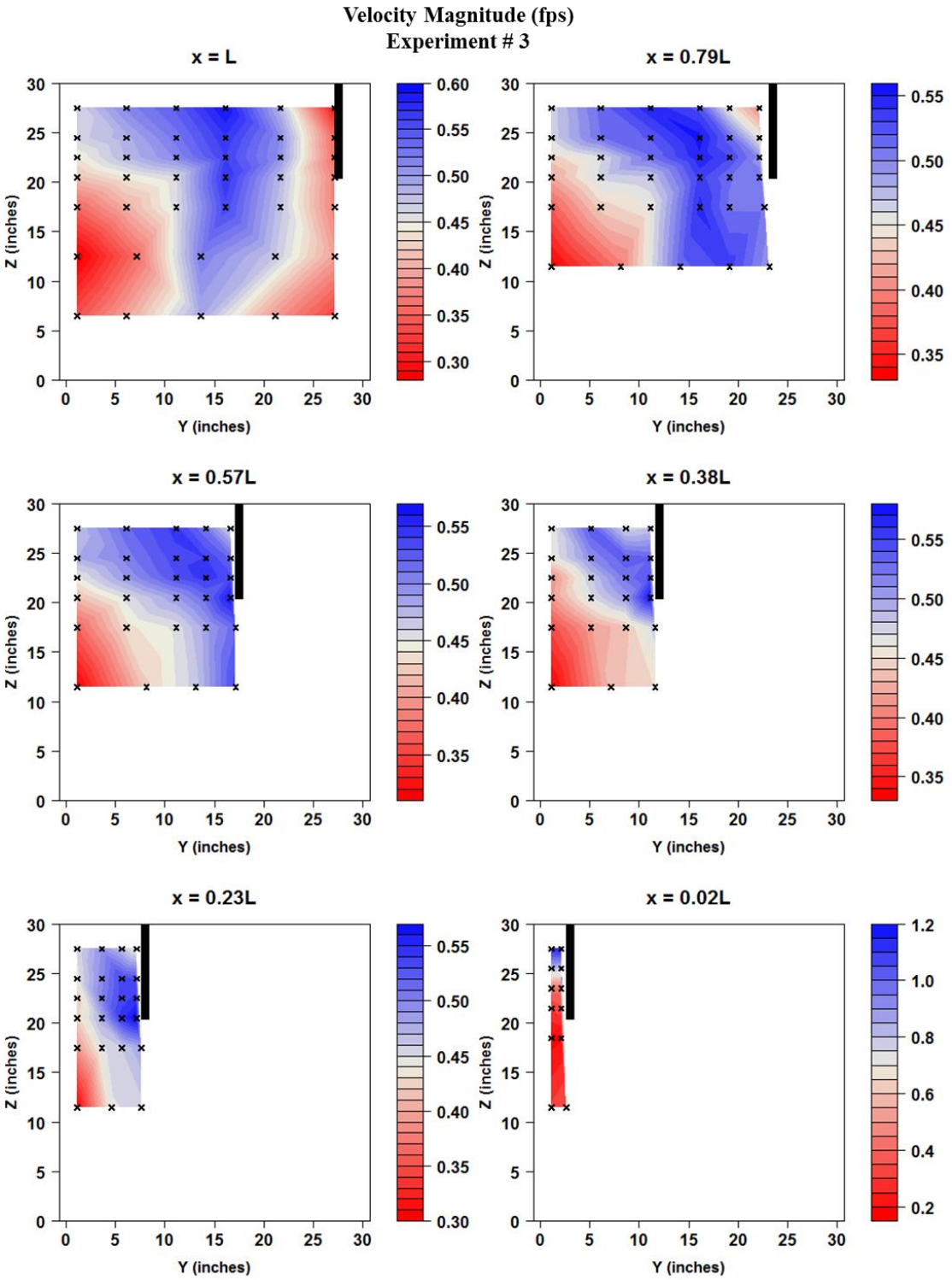

Figure 19: Velocity Magnitude for Experiment 3. The black "x's" indicate the location of each data point. Values were interpolated between each data point assuming a linear relationship. The black rectangle indicates the location of the guide wall in relation to the cross-section.

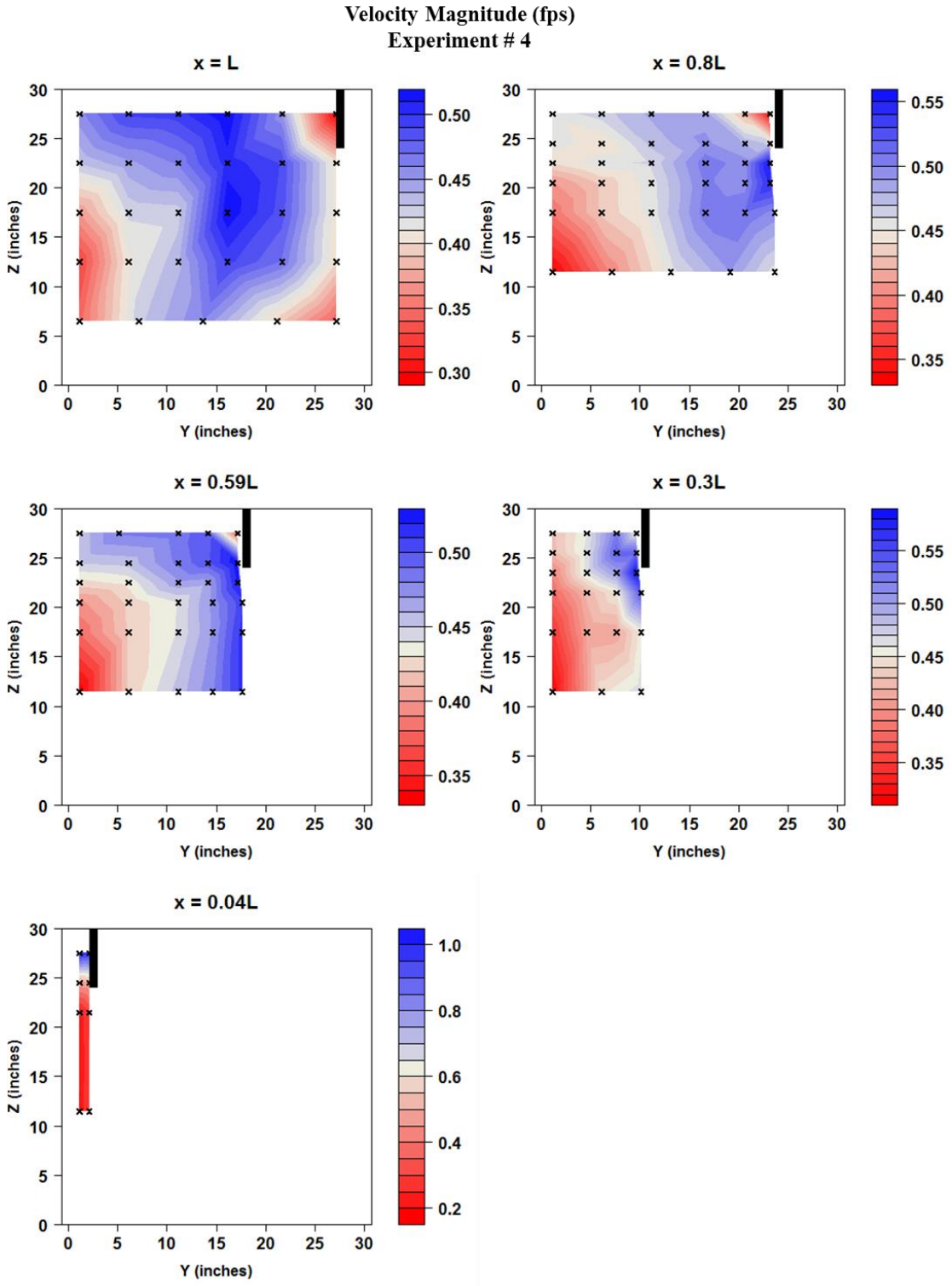

Figure 20: Velocity Magnitude for Experiment 4. The black "x's" indicate the location of each data point. Values were interpolated between each data point assuming a linear relationship. The black rectangle indicates the location of the guide wall in relation to the cross-section.

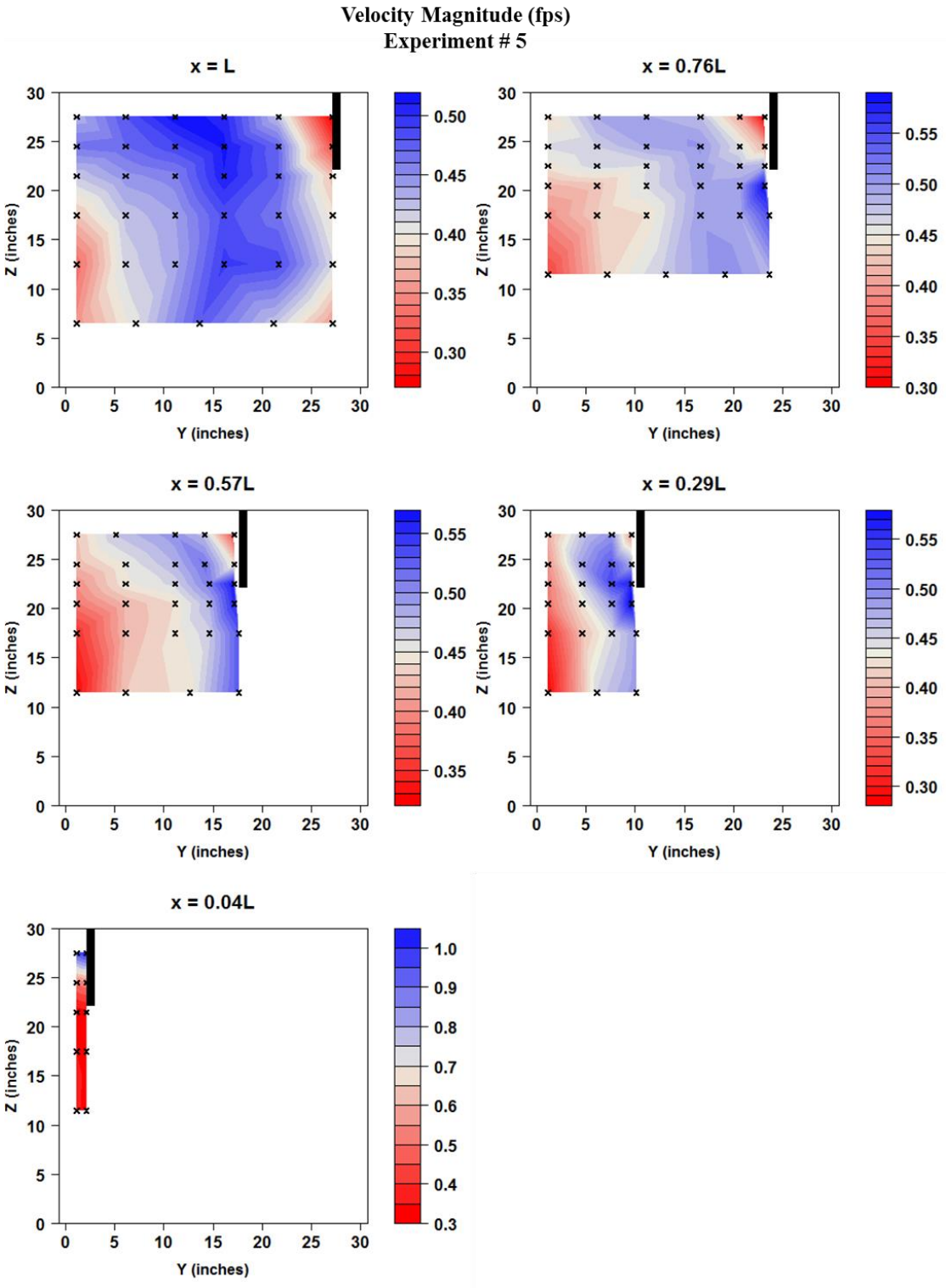

Figure 21: Velocity Magnitude for Experiment 5. The black "x's" indicate the location of each data point. Values were interpolated between each data point assuming a linear relationship. The black rectangle indicates the location of the guide wall in relation to the cross-section.

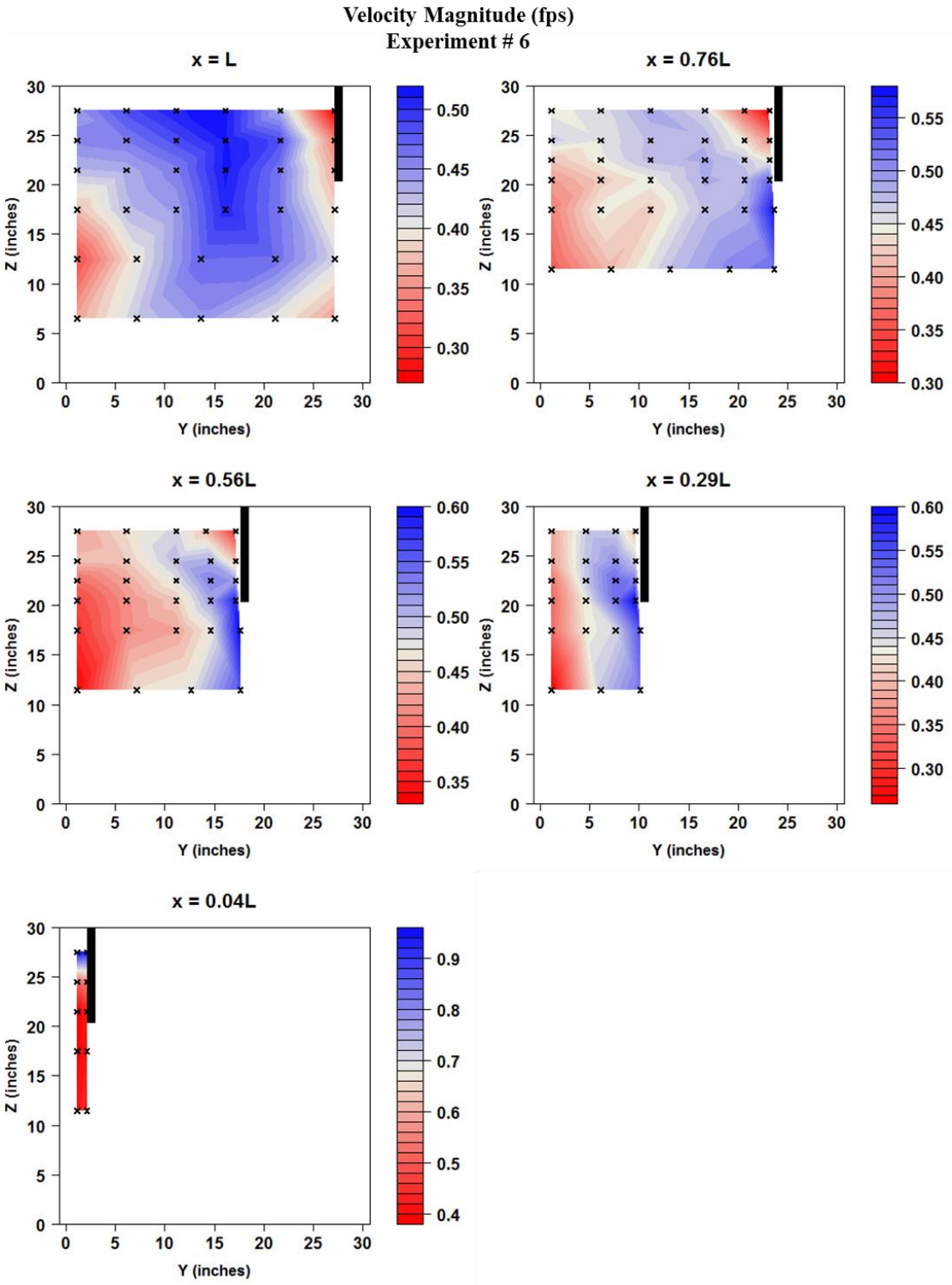

Figure 22: Velocity Magnitude for Experiment 6. The black "x's" indicate the location of each data point. Values were interpolated between each data point assuming a linear relationship. The black rectangle indicates the location of the guide wall in relation to the cross-section.

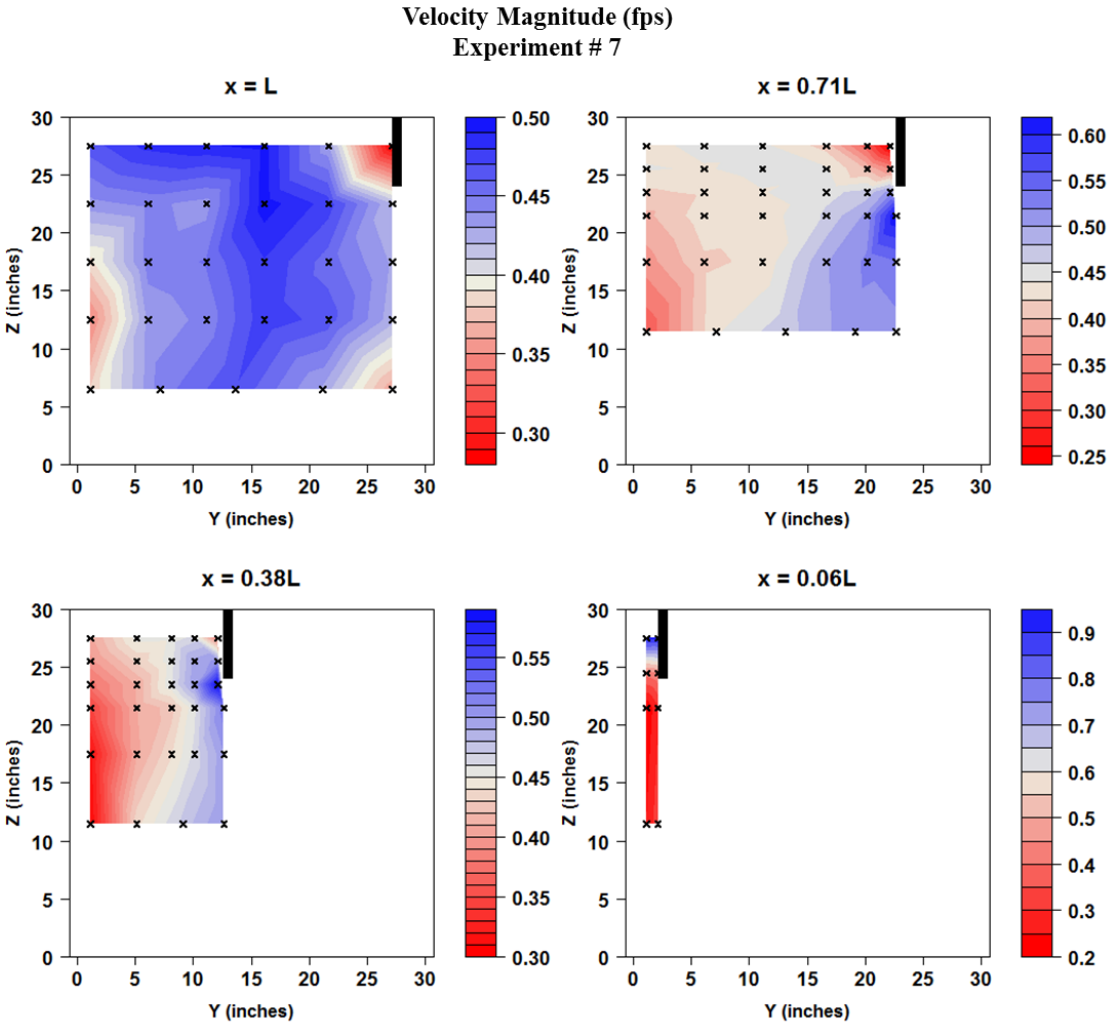

Figure 23: Velocity Magnitude for Experiment 7. The black "x's" indicate the location of each data point. Values were interpolated between each data point assuming a linear relationship. The black rectangle indicates the location of the guide wall in relation to the cross-section.

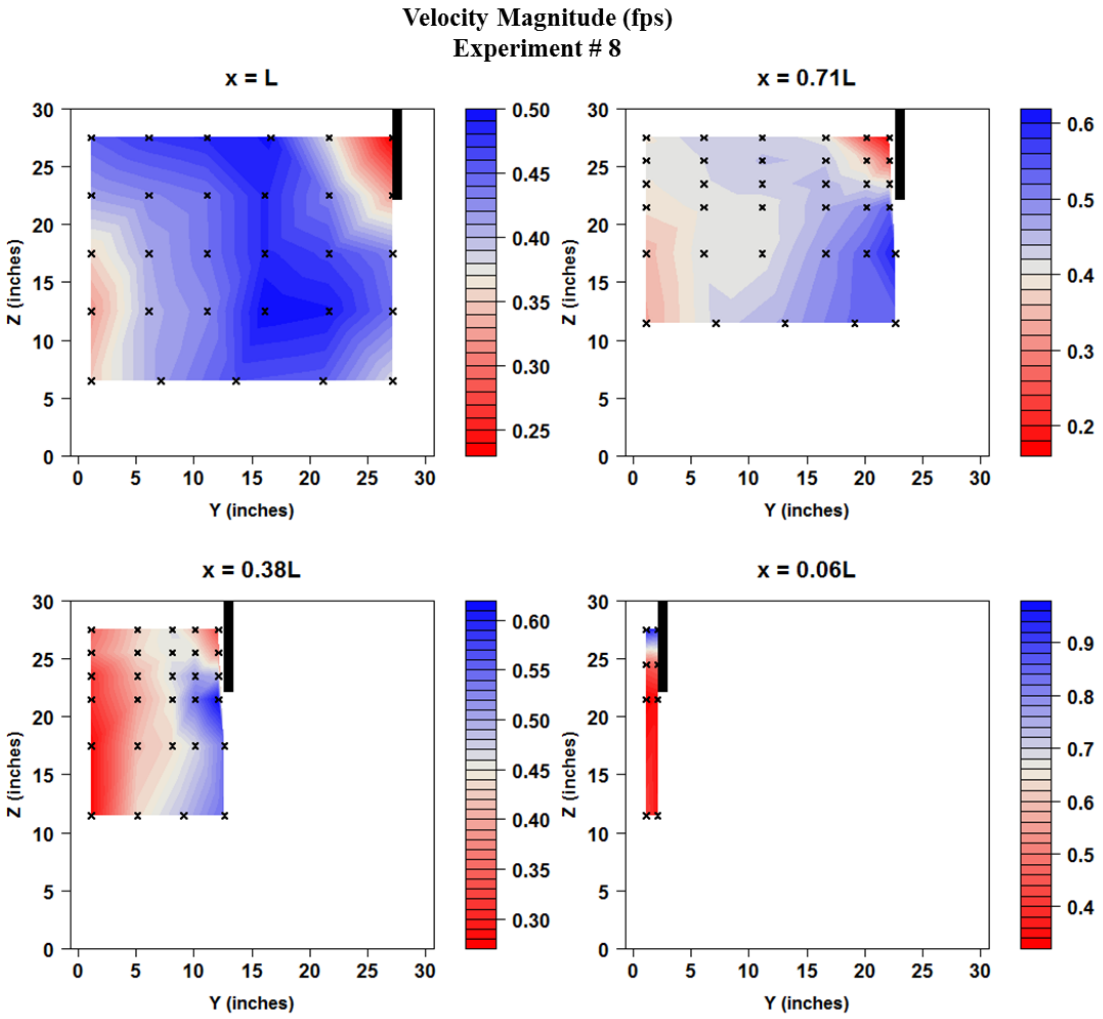

Figure 24: Velocity Magnitude for Experiment 8. The black "x's" indicate the location of each data point. Values were interpolated between each data point assuming a linear relationship. The black rectangle indicates the location of the guide wall in relation to the cross-section.

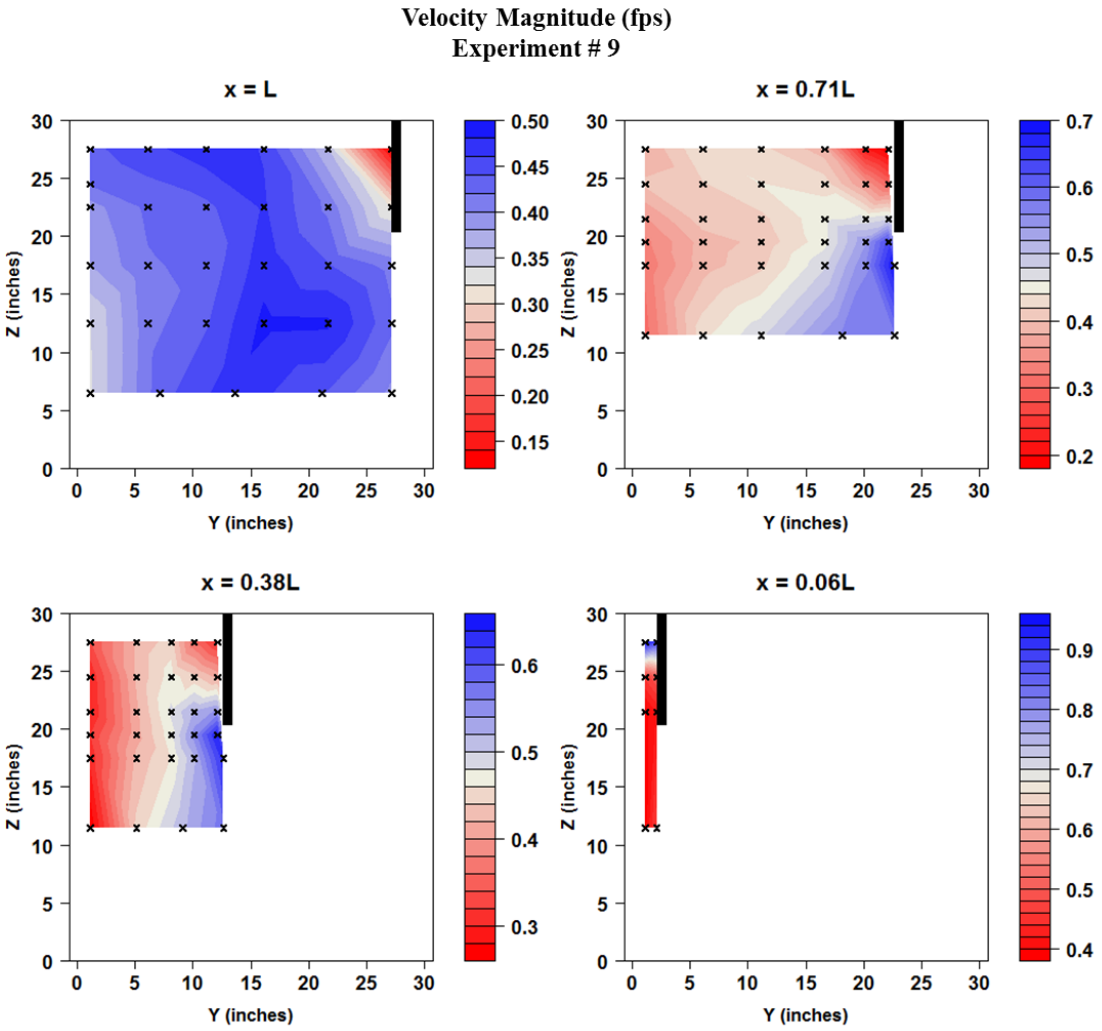

Figure 25: Velocity Magnitude for Experiment 9. The black "x's" indicate the location of each data point. Values were interpolated between each data point assuming a linear relationship. The black rectangle indicates the location of the guide wall in relation to the cross-section.

Chapter 3: Improvements to floating impermeable guidance structures for downstream fish passage

1. Proposed Work

In Chapter 3 we will determine whether or not an apron (Fig. 1) placed at the bottom of a guide wall could help to improve guidance efficiencies. We plan to compare the physical modelling results of Chapter 2 (without the apron) to a set of configurations with an apron of different shapes and sizes. The same measures will be used to quantify the flow field as performed in Chapter 2. The following configurations will be tested (values are in prototype scale):

- FIGS Depth, d = 16.67'
- FIGS Angle, θ = 45°
- Average Approach Velocity, V = 2 fps, 2.5 fps, 3 fps
- Percent of Flow Through the Bypass, p = 5%
- Apron Length, a = 0', 2', 4'

This results in 9 total scenarios using the "worst-case" depth and angle of the structure. We will examine the effect of the Average Approach Velocity on both the velocity magnitude and the Z-Velocity Ratio upstream of the guide wall. The test will be completed both without (a = 0') and with (a = 2', 4') an apron. The scenario where V = 2fps and a = 0' has already been completed in Chapter 2.

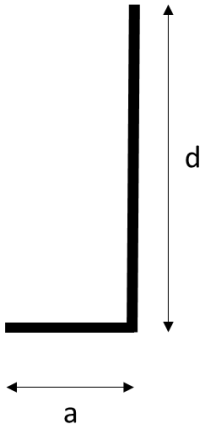

Figure 1: The schematic shows the side view of the apron and guide wall. The apron length (a) is depicted in relation to the depth of the guide wall (d).